Distinct adaptation and epidemiological success of different genotypes within *Salmonella enterica* serovar Dublin

Cheryll M Sia[1,2*], Rebecca L Ambrose[3], Mary Valcanis[2], Patiyan Andersson[2], Susan A Ballard[2], Benjamin P Howden[1,2], Deborah A Williamson[4#], Jaclyn S Pearson[3,5,6*#], Danielle J Ingle [1*#]

[1] *Department of Microbiology and Immunology, The University of Melbourne at The Peter Doherty Institute for Infection and Immunity, Melbourne, 3000, Victoria, Australia.*

[2] *Microbiological Diagnostic Unit Public Health Laboratory, Department of Microbiology & Immunology, The University of Melbourne at The Peter Doherty Institute for Infection and Immunity, Melbourne, 3000, Victoria, Australia.*

[3] *Centre for Innate Immunity and Infectious Diseases, Hudson Institute of Medical Research, Clayton, 3168, Victoria, Australia.*

[4] *Department of Infectious Diseases, The University of Melbourne at the Peter Doherty Institute for Infection and Immunity, Melbourne, 3000, Victoria, Australia.*

[5] *Department of Microbiology, Monash University, Clayton, 3168, Victoria, Australia.*

[6] *School of Medicine, University of St Andrews, St Andrews, KY16 9TF, Fife, United Kingdom.*

 # Contributed equally

*** Corresponding author**

CMS: cmsia@unimelb.edu.au

JSP: jp287@st-andrews.ac.uk

DJI: danielle.ingle@unimelb.edu.au

ABSTRACT

Salmonella Dublin is a host-adapted, invasive non-typhoidal *Salmonella* (iNTS) serovar that causes bloodstream infections in humans and demonstrates increasing prevalence of antimicrobial resistance (AMR). Using a global dataset of 1,303 genomes, coupled with *in vitro* assays, we examined the evolutionary, resistance, and virulence characteristics of *S*. Dublin. Our analysis revealed strong geographic associations between AMR profiles and plasmid types, with highly resistant isolates confined predominantly to North America, linked to IncC plasmids co-encoding AMR and heavy metal resistance. By contrast, Australian isolates were largely antimicrobial-susceptible, reflecting differing AMR pressures. We identified two phylogenetically distinct Australian lineages, ST10 and ST74, with a small number of ST10 isolates harbouring a novel hybrid plasmid encoding both AMR and mercuric resistance. Whereas the ST10 lineage remains globally dominant, the ST74 lineage was less prevalent. ST74 exhibited unique genomic features including a larger pan genome compared to ST10 and the absence of key virulence loci including SPI-19 which encodes a type VI secretion system (T6SS). Despite these genomic differences, the ST74 lineage displayed enhanced intracellular replication in human macrophages and induced less pro-inflammatory responses compared with ST10, suggesting alternative virulence strategies that may support systemic dissemination of ST74. The Vi antigen was absent in all ST10 and ST74 genomes, highlighting challenges for serotyping and vaccine development, and has implications for current diagnostic and control strategies for *S.* Dublin infections. Collectively, this study represents the most comprehensive investigation of *S*. Dublin to date and importantly, has revealed distinct adaptations of two genotypes within the same serovar, leading to different epidemiological success. The regional emergence and evolution of distinct *S.* Dublin lineages highlights the need to understand the divergence of intra-serovar virulence mechanisms which may impact the development of effective control measures against this important global pathogen.

Funding

DAW was supported by a National Health and Medical Research Council (NHMRC) Investigator Grant (GNT1174555) and a Medical Research Future Fund (MRFF) Grant (FSPGN000045). BPH is supported by NHMRC Investigator Grant (GNT1196103). DJI is supported by an NHMRC Investigator Grant (GNT1195210). JSP was supported by a Sylvia and Charles Viertel Senior Medical Fellowship. MDU PHL is funded by the Victorian Government, Australia. No conflict of interest declared.

Keywords

Invasive nontyphoidal *Salmonella*, antimicrobial resistance, heavy metal resistance, virulence; One Health

64 **INTRODUCTION**

65 Invasive nontyphoidal *Salmonella* (iNTS) infections are a major cause of global morbidity and
66 mortality (1). Of the >2,500 NTS serovars, iNTS infections are associated with a relatively
67 limited number of serovars. These include *Salmonella enterica* serovar Dublin (*S.* Dublin), *S.*
68 Panama, *S.* Virchow, *S.* Choleraesuis and *S.* Typhimurium ST313 (2–4). *S.* Dublin, a bovine-
69 adapted pathogen, is one of the leading iNTS serovars both in Australia and globally (5–7), and
70 is associated with bacteraemia in a high proportion of infections (2,5–7). Symptomatic cattle
71 may develop septicaemia and transplacental transmission (7,8), while asymptomatic infections
72 in cattle enable persistence within the herd population, facilitating disease spread (7,9). *S.*
73 Dublin causes zoonotic infections predominately through the consumption of contaminated
74 dairy and meat produce (10–12), and as such is considered a 'One Health' pathogen. (10–12).
75

76 Antimicrobial resistance (AMR) in NTS has increased over the past several decades, leading
77 to the reduction of therapeutic options (6,13). Although *S.* Dublin isolates are largely
78 susceptible to therapeutics, AMR has become increasingly prevalent in *S.* Dublin (7,12,14–16).
79 For example, a multidrug-resistant (MDR; defined as resistance to ≥ 3 antimicrobial classes
80 (17)) lineage has recently been described in North America, characterised by varying profiles
81 of AMR to ampicillin, streptomycin, chloramphenicol, sulphonamides, tetracyclines and third
82 generation cephalosporins. These MDR *S.* Dublin isolates all type as sequence type 10 (ST10),
83 and the AMR determinants have been demonstrated to be carried on an IncC plasmid that has
84 recombined with a virulence plasmid encoding the *spvRABCD* operon (7,12,16,18). This has
85 resulted in hybrid virulence and AMR plasmids circulating in North America including a 329kb
86 megaplasmid with IncX1, IncFIA, IncFIB and IncFII replicons (isolate CVM22429, NCBI
87 accession CP032397.1) (12,16) and a smaller hybrid plasmid 172,265 bases in size with an
88 IncX1 replicon (isolate N13-01125, NCBI accession KX815983.1) (18).

89

90 *S.* Dublin is closely related to *S.* Enteritidis and *S.* Gallinarum (19), with differences in
91 accessory genome content reflective of adaptation to different ecological niches (19). The
92 majority of the STs reported for *S.* Dublin are ST10 or single-locus variants of this ST, although
93 there is a second lineage, ST74, that is distinct from the main *S.* Dublin population (20). This
94 uncommon *S.* Dublin lineage, ST74, may be variably serotyped as *S.* Dublin or *S.* Enteritidis
95 dependent upon the strains used to generate typing sera in different laboratories (20), which
96 may have also contributed to it not being identified. The antigenic formula of *S.* Dublin
97 (1,9,12:g,p:-) is highly similar to *S.* Enteritidis (1,9,12:g,m:-), with three non-synonymous
98 point mutations in *fliC* (Ala220Val, Thr315Ilc and Thr318Ala) differentiating the two serovars.
99 Although the Vi capsular antigen (encoded by the *viaB* locus) is part of the antigenic definition
100 for *S*. Dublin, it has been shown that the Vi antigen is absent in many *S.* Dublin isolates (20,21).
101 Other putative virulence determinants in *S.* Dublin include *Salmonella* pathogenicity islands
102 (SPIs) 6 and 19, which both encode type VI secretion system (T6SS) machineries (22,23). The
103 presence of two T6SSs in *S*. Dublin contrasts with other NTS serovars, which encode a single
104 T6SS (22,23). T6SSs are molecular nanomachines that deliver effector proteins into eukaryotic
105 and/or prokaryotic cells to promote pathogen survival within multispecies and complex
106 immune environments such as the gut. Recent studies have demonstrated a role for SPI-6 and
107 SPI-19 in interbacterial competition by specific *S.* Dublin strains (24,25), however their effect
108 on host immune processes remains largely unknown.

109

110 We previously undertook a genomic investigation of another emerging NTS lineage in
111 Australia, *Salmonella enterica* serovar 4,[5],12:i:-, and identified several bacterial traits that
112 may have contributed to the successful spread of this lineage (26–30). In particular, we
113 hypothesised that flagellin deletion and MDR status may have contributed to host immune

114 evasion and positive selection, respectively, in *Salmonella enterica* serovar 4,[5],12:i:- (31).
115 Here, we sought to understand the contribution of virulence and resistance to the recent
116 emergence of MDR *S.* Dublin. We interrogated a global dataset of 1,303 isolates collected
117 from 13 countries on five continents and identified distinct geographical lineages associated
118 with specific AMR and virulence profiles, including a lineage unique with increased capability
119 for intracellular survival and immune evasion in human macrophages.
120

121 **RESULTS**

122 ***Distinct S. Dublin populations circulate globally***

123 A total of 1,303 *S.* Dublin genomes were included in our analysis, spanning four decades
124 (Figure 1A, Supplementary Tables 1-2). This dataset included 53 genomes from humans in
125 Australia, and 1,250 genomes from Africa, Europe, North and South America collected from
126 humans (*n*=462), animals (*n*=551), food (*n*=223) and other sources that were not stated (*n*=67)
127 (Figure 1B, Supplementary Tables 1-2). In total, 1,235 genomes (99.4%) were ST10 and 58
128 were a single locus variant (SLV) of ST10, with two double locus variant genomes (e.g.
129 ST4100) restricted to isolates from South America. The exceptions were ST74 and SLV
130 ST1545 that were only detected in Australia (Figure 1C-E, Supplementary Table 3). All
131 isolates, including the ST74 lineage, were serotyped *in silico* as *S.* Dublin. However, the ST74
132 lineage and a single ST10 isolate had codon profiles in *fliC* of Gly60, Leu138, Ala220, Thr315
133 and Ala318, in contrast to the remaining ST10 and SLV, which both had a profile of Gly60,
134 Leu138, Val220, Ile315 and Ala318 (the previously described 'Du2' and 'Du1' electrophoretic
135 profiles (21), respectively) (Supplementary Table 4).
136

137 A maximum likelihood (ML) phylogeny was inferred from the 1,303 genomes, revealing two
138 major lineages of *S.* Dublin, ST74 and ST10 (Figure 1D, Supplementary Figure 1). Within the

139 ST10 lineage, five clades were identified using Bayesian Analysis of Population Structure
140 (BAPS), inferred from the alignment of 2,957 core single nucleotide polymorphisms (SNPs).
141 Four clades were broadly associated with geographical region (Supplementary Figure 1,
142 Supplementary Table 1). The Australian ST10 isolates (n = 39) clustered in clade 1, while
143 isolates from North America were associated with clade 5 (Supplementary Figure 1). The
144 BAPS clade 2 were the isolates that didn't have sufficient evidence to be split into further
145 clades, hence are spread across the tree spanning a range of geographical regions.
146
147 ***Emergence of S. Dublin lineages in the 20th century***
148 To investigate the emergence of *S.* Dublin clades, Bayesian phylodynamic analysis was
149 undertaken on a representative subset of 660 genomes, selected for phylogenetic, geographical
150 and AMR diversity (see methods). We inferred a maximum clade credibility (MCC) phylogeny
151 from an alignment of 3,971 SNPs using the highest supported model of a relaxed lognormal
152 molecular clock and coalescent exponential tree prior. The estimated substitution rate was 1.05
153 x 10^{-7} (95% highest posterior density (HPD): 1.16 x 10^{-7}– 9.41 x 10^{-8}), slightly higher than
154 previous estimated mean substitution rates for host-restricted *Salmonella* serovars (*S.* Typhi
155 and *S.* Paratyphi A) but lower than rates reported for host-generalist NTS serovars *S.* Kentucky
156 and *S.* Agona (32).
157
158 The topology of the MCC tree was consistent with the ML tree, with geographically associated
159 sub-clades were observed in the MCC tree (Figure 2, interactive tree is available in Microreact
160 under https://microreact.org/project/sdublinpaper). The most recent common ancestor
161 (MRCA) for the *S.* Dublin global population was inferred to be 1901 (HPD 1878-1924), with
162 the MRCA of the different clades and sub-clades largely falling between 1950 and 2000. For
163 example, the most recent common ancestor (MRCA) of clade 5 MDR isolates from North

164 America was estimated to be ~1964 (HPD 1952 -1974) (Figure 2). The MRCA of the Australian
165 sub-clade was estimated to be ~1967 (HPD 1953-1980); with the Australian and North
166 American isolates inferred to have a MRCA ~1931 (HPD 1914-1947). Moreover, three clades
167 (1, 3, and 4) had European sub-clades associated with Sweden, the UK, and Denmark,
168 respectively that were all largely susceptible to antimicrobials. Some regions, such as Europe
169 and South America, were associated with several sub-clades of *S.* Dublin, potentially
170 suggesting multiple importations and expansions, while other regions, such as Australia were
171 comprised of a single sub-clade within clade 1.
172
173 ***Resistance determinants are associated with geographical regions***
174 Different plasmid types co-occurred with different AMR and HMR determinants in the *S.*
175 Dublin population, and these were also associated with differential geographical distribution
176 (Figure 2, Supplementary Figure 3-4, Supplementary Table 1). Overall, 51.5% (667/1,295) of
177 *S.* Dublin genomes had at least one AMR determinant, with 632/667 (94.8%) isolates classified
178 as MDR. MDR *S.* Dublin was predominantly identified from North American isolates, although
179 some AMR determinants were detected in *S.* Dublin from other geographic regions (Figure 3,
180 Supplementary Figures 2-3). AMR *S.* Dublin collected from animals was common
181 (*n*=305/667; 45.7%). AMR in *S.* Dublin from food sources and humans was similar in
182 proportion (*n*=174/667; 26.1% and *n*=173/667; 25.9% respectively). Although these profiles
183 are likely impacted by the sampling frame of different studies, the source of collection was not
184 considered as a selection criterion for this study, and as such, may broadly represent the AMR
185 profiles of *S.* Dublin from different sources (Figure 3A-B, Supplementary Figure 1).
186
187 The most prevalent AMR determinants were *strA-B* (*n*=620), *floR* (*n*=556), *tet*(A) (*n*=608) and
188 *sul2* (*n*=596) (Supplementary Figure 2). AMR mechanisms to ciprofloxacin (triple point

189 mutations in quinolone resistance determining regions *gyrA*[83:S-F], *gyrA*[87:D-N],
190 *parC*[80:S-I]), macrolides (*mph*(A)), and colistin (*mcr-9.1*) were each detected in single
191 genomes from *S.* Dublin clade 5 at a low frequency of 0.08% (*n*=1/1,303) in the dataset. The
192 only third generation cephalosporin (3GC) resistance mechanism detected was $bla_{\text{CMY-2}}$,
193 present in 467/667 (70%) of AMR *S.* Dublin genomes. Although *strA-B*, *tet*(A) and $bla_{\text{TEM-1}}$
194 were observed in multiple clades, *floR*, *sul2* and $bla_{\text{CMY-2}}$ were restricted to North American
195 isolates that fell in clade 5 (Supplementary Figure 2-3). This MDR profile, in addition to *strA-*
196 *strB* and *tet*(A), was mediated by IncC plasmids in 593 genomes (*n*=509 from the United States
197 of America [USA], *n*=82 from Canada and *n*=2 from the UK) (Supplementary Figure 3, 4C).
198 Nearly all clade 3 isolates linked to the UK had no AMR determinants, except for four isolates
199 collected between 2010-2015 (Supplementary Figure 1-3, Figure 3, Supplementary Table 1).
200
201 In addition to AMR determinants, we characterised biocide and heavy metal resistance (HMR)
202 profiles of the *S.* Dublin isolates. Gold resistance determinants *golS* and *golT* were ubiquitous
203 in *S.* Dublin (*n*=1,302/1,303; 99.9%) (Figure 3C, Supplementary Figures 2-3). Consistent with
204 previous findings biocide and HMR determinants, including *qacEdelta1* and mercury
205 resistance genes (*merABDEPRT*), commonly co-occurred with AMR determinants. Notably,
206 the *mer* operon was frequently associated with the IncC MDR plasmid (90.1%; *n*=534/593)
207 (Supplementary Figure 3, Supplementary Table 1).
208
209 ***Characterisation of S. Dublin plasmids and identification of a novel hybrid plasmid***
210 Both IncX1 (*n*=1269/1303; 97.4%) and IncFII(S) (*n*=1213/1303; 93.1%) plasmid replicons
211 were found at high frequency within the dataset, in line with previous findings (12). Three
212 plasmid replicons, namely IncN, IncX1 and IncFII(S), and a MOBF/MOBP relaxase, were
213 detected in one of the Australian *S.* Dublin ST10 genomes from clade 1 (AUSMDU00035676).

214 Comparative analysis revealed the AUSMDU00035676 plasmid lacked the *spv* operon and had
215 low homology to reference IncN and IncX1/IncFII(S) plasmids previously associated with
216 *Salmonella* (Supplementary Figure 5, Supplementary Table 5). The loss of the *spv* operon may
217 be associated with a less invasive phenotype (33). This finding suggests the detection of a
218 potentially novel hybrid plasmid with IncN/IncX1/IncFII(S) markers that encodes AMR and
219 HMR determinants flanked by IS26 elements, which may aid gene mobilisation (34). In
220 contrast, the AUSMDU00056868 plasmid had IncX1/IncFII(S) plasmid replicon markers and
221 was found to not encode any mechanisms for resistance. This plasmid was >99% homologous
222 to known virulence reference *S.* Dublin plasmids pOU1115 and pSDU2_USMARC_69807 and
223 encoded the *spv* operon (Supplementary Table 5, Supplementary Figure 6). This suggests that
224 the *S.* Dublin virulence plasmid is conserved, while the *spv* operon that has been shown to
225 enhance disease severity (14,16,35–37) is maintained on the plasmid. Complete annotations of
226 both AUSMDU00035676 and AUSMDU00056868 can be found in Supplementary Tables 6
227 and 7, respectively.
228
229 ***Diversity in virulence determinants across S.* Dublin lineages**
230 To investigate the potential for invasiveness within *S.* Dublin, we applied a previously
231 described bioinformatic tool to our dataset of 1,303 *S.* Dublin genomes (38). In brief, this tool
232 infers the likelihood of invasiveness by assigning an index score between 0 to 1 that reflects
233 the level of genome degradation, whereby a higher score suggests genomic features that may
234 be more associated with a narrower host range and great likelihood of invasiveness (38). We
235 performed initial validation work using 36 complete publicly available reference genomes,
236 covering known invasive and non-invasive phenotypes (Supplementary Table 8). Using this
237 validation set, invasive and largely host-restricted serovars, including *S.* Choleraesuis, *S.*
238 Paratyphi and *S.* Typhi, scored >0.5, suggestive of an invasive genomic profile (Figure 4A,

239 Supplementary Table 8). Conversely, non-invasive NTS serovars with broader ecological
240 niches, including *S*. Anatum, ST19 *S*. Typhimurium and *S.* Derby, scored <0.5 (Figure 4A,
241 Supplementary Table 8). When applied to our *S.* Dublin dataset, only eleven genomes
242 (*n*=11/1,303; 0.84%) had an index score < 0.5. These included three ST10 genomes and all
243 eight ST74 genomes (Figure 4B, Supplementary Table 9). Based on descriptive analysis, no
244 apparent relationship was observed between index scores and region or source attribution
245 (Figure 4B).
246
247 Putative virulence determinants identified in *S*. Dublin genomes included SPIs, the *spv* operon
248 (16), prophages and other individual genes (Supplementary Table 9). Some putative virulence
249 factors, such as *pagN* [cell adhesion and invasion (39,40)] and *pgtE,* [virulence (27,41)], were
250 found in 1,303 (100%, *n*=1,303/1,303) and 1,302 (99.9%, *n*=1,302/1,303) genomes
251 respectively, and no SNPs in the promoter region of *pgtE* were detected, a mutation previously
252 reported in invasive *S*. Typhimurium ST313 (27). In contrast, ST313-gi of unknown function
253 (27,41), the Gifsy-2 like prophage [unknown function (27,41)] and *ggt* gene thought to be
254 involved in gut colonisation (35), were detected in the major ST10 *S.* Dublin lineages, and
255 absent in ST74 *S.* Dublin. The *viaB* operon encoding the Vi capsular antigen was only detected
256 in SLV ST73, a historical isolate from France that displayed the Du3 electrophoretic type that
257 was consistent with a previous study (21). This suggests that the Vi antigen is not conserved in
258 the *S.* Dublin population or associated with virulence.
259
260 The presence of SPI-6 and SPI-19 differed across *S.* Dublin isolates. Both SPIs encode T6SSs
261 that provide a means for injecting effector proteins into adjacent competing bacteria or host
262 cells for immune evasion (23,42). SPI-19 was absent in the ST74 *S.* Dublin lineage but present
263 in all ST10 *S.* Dublin (Supplementary Figure 7). The genetic differences between ST74 and

264 ST10 were reflected in the disparity of their index scores of <0.5 and >0.5, respectively. The
265 SPI-6 region was detected in all isolates, however <90% sequence coverage was detected in
266 422/1,303 genomes (32.4%). Long read sequencing on three genomes of the ST74 lineage and
267 three genomes from the ST10 clade 1 lineage corroborated these findings (Figure 4C-E),
268 demonstrating truncation of SPI-6 with the T6SS machinery (Figure 4D). Long-read
269 sequencing also revealed an absence of SPI-19 in the three ST74 isolates and presence of SPI-
270 19 in the three ST10 isolates (Figure 4C, E). The absence of SPI-19 in ST74 suggests that this
271 deletion event occurred during its divergence from the primary *S*. Dublin lineage, ST10.
272
273 ***Infection of human macrophages reveals distinct intracellular replication patterns between***
274 ***ST10 and ST74 lineages***
275 Given the distinct genomic profiles of ST10 and ST74 lineages, we compared the phenotypic
276 profile of a selection of Australian isolates from each lineage *in vitro*. The immortalised human
277 macrophage cell line, THP-1, was used to assess invasion, intracellular replication and host
278 cytotoxicity induced by a subset of clinical isolates from the two lineages. Specifically, we
279 assayed an ST10 population comprising eleven isolates, including an isolate from the highly
280 related ST4293 lineage, and an ST74 population comprising seven isolates including an isolate
281 from the highly related ST1545 lineage (Supplementary Table 10). Although predicted invasive
282 index scores were higher for the ST10 population (Figure 4B), each isolate failed to replicate
283 more than 2-fold over 24 hours in THP-1 cells (Figure 5A), whereas isolates within the ST74
284 population displayed a sustained increase in fold change of intracellular replication, up to 8-
285 fold, over 24 hours (Figure 5B). Comparing bacterial growth (CFU/ml) across both sequence
286 types, both lineages were comparable for initial bacterial uptake (Figure 5C) however, the ST74
287 population replicated to significantly higher levels in THP-1 macrophages at 9- and 24-hours
288 post-infection (hpi) compared to the ST10 population (Figure 5D-F). Given that NTS also

289 replicate in epithelial cells, we utilised an immortalised human intestinal epithelial cell line,
290 HT-29, to assess *S.* Dublin replication. In contrast to the results obtained in macrophages, we
291 found that 6 out of 11 isolates within the ST10 population replicated more efficiently (up to
292 10-fold) in HT-29 cells, whereas all seven isolates within the ST74 population showed minimal
293 replication (up to 2-fold) over 24 hours (Supplementary Figure 8A-C).
294
295 ***Increased replication of ST74 isolates in human macrophages does not correlate with***
296 ***increased host cell death***
297 It is well documented that protype *S.* Typhimurium (ST19) potently induce macrophage
298 cytotoxicity both *in vitro* and *in vivo* (43). Here, we utilised a cellular lactate dehydrogenase
299 (LDH) release assay to assess THP-1 cytotoxicity in response to infection with *S.* Dublin ST74
300 and ST10 populations. Surprisingly, the substantial intracellular replication of the ST74
301 population in THP-1 cells induced significantly less host cell cytotoxicity at 3 and 9 hpi
302 compared with the ST10 population suggesting potential immune evasion by ST74 (Figure 6A,
303 B). By 24 hpi however, cytotoxicity induced by both ST74 and ST10 populations was relatively
304 high, with no significant difference observed across the sequence types (Figure 6C). In contrast,
305 there was minimal cytotoxicity observed in infected HT-29 cells across the board
306 (Supplementary Figure 8D), suggesting a less potent activation of host cell death in infected
307 epithelial cells compared with macrophages.
308
309 To understand how the ST74 population may be supressing macrophage death at earlier stages
310 of infection, we measured protein secretion of IL-1ß via cytokine release and immunoblot
311 assays at 9 hpi, respectively. IL-1ß is a potent pro-inflammatory cytokine that is released upon
312 activation of the NLRC4 inflammasome by components of the *Salmonella* type III secretion
313 apparatus (44), resulting in a lytic cell death process known as pyroptosis (45). Here, we

observed significantly less IL-1ß release by THP-1 cells infected with isolates from the ST74 population at 9 hpi compared with those from the ST10 population (Figure 6D), directly reflecting the LDH cytotoxicity data represented in Figure 6B. To further support our observations, we selected single representative isolates of ST74 and ST10 to perform immunoblot analyses of cleaved IL-1ß (activated form) within THP-1 cells. Here, ST74 induced less IL-1ß cleavage at 9 hpi compared to the ST10 (Figure 6E). We included the ubiquitous laboratory NTS reference strain, *S.* Typhimurium SL1344 in the immunoblot analysis as this is known to potently induce pyroptosis in human macrophages (46). As expected, SL1344 induced significant IL-1ß cleavage during infection of THP-1 macrophages (Figure 6E). To assess the correlation of cellular cytotoxicity as measured by LDH, IL-1ß release and intracellular replication, we generated a scatter plot of all isolates within the ST74 and ST10 populations. Here we can clearly demonstrate that isolates from the ST74 population have increased replicative ability, induce less cytotoxicity, and lower levels of IL-1ß release (Figure 6F) compared with those within the ST10 population. There were however, some ST10 isolates that induced similarly low levels of host cell death, presumably due to lower levels of intracellular replication (Figure 6F and Supplementary Figure 9A, B). These isolates generally clustered away from the ST10 isolates that induced more cell death (Supplementary Figure 9C).

A pangenome analysis of the isolates from both ST10 and ST74 lineages revealed that out of a total of 5,792 genes, there were 473 and 1,143 genes specific to the ST10 and ST74 lineage, respectively (Supplementary Figure 10, Supplementary Table 11). Further, out of 1,143 genes, there were 362 core genes present in all isolates from the ST74 lineage (Supplementary Table 11). To highlight these differences, an SNP distance matrix was generated, revealing a minimum of 2,402 SNPs between the ST10 and ST74 lineages (Supplementary Table 12).

339 While these findings require further investigation, an increased gene content and genome size
340 were consistently observed in all isolates of the ST74 lineage (Supplementary Tables 11 and
341 13). These results indicate a potential link between the unique genome content of the ST74
342 lineage and alterations in host responses and replicative ability.
343
344 **DISCUSSION**
345 Our data provide comprehensive insights into the emergence and spread of *S*. Dublin, with
346 distinct geographic distribution related to AMR and virulence. Analysing the largest global
347 dataset of *S*. Dublin genomes to date, we show that highly resistant *S.* Dublin is almost entirely
348 confined to North America, with emergence in the late 20th century and ongoing local
349 microevolution. Consistent with previous studies, the North American *S.* Dublin isolates in
350 clade 5 were characterised by the presence of an IncC plasmid, often with co-location of AMR
351 and HMR determinants (16,18), while the clades circulating in Europe were associated with
352 IncN plasmids (47). Previous studies have explored these IncC plasmids in detail. The use of
353 biocides and heavy metals in the agri-food industry may facilitate co-selection, contributing to
354 the persistence of AMR (48). This highlights the potential for selection pressure in one
355 ecological niche (e.g. the use of biocides in farming or heavy metals in animal feeds) leading
356 to AMR in another (e.g. AMR in humans).
357
358 The phylogeographic separation, AMR and plasmid profiles of *S.* Dublin lineages is consistent
359 with other studies (7,12,49–53),, and is likely to be influenced by several factors, including
360 local AMR use and patterns of livestock movement. Given the livestock reservoir of *S.* Dublin
361 is mostly host-restricted to cattle, it is conceivable that both historic and contemporary global
362 cattle movement may have contributed to region-specific differences in *S.* Dublin. For
363 example, Australian *S.* Dublin genomes in clade 1 shared a common ancestor with North

364 American isolates in clade 5. During the early 1930's, Brahman cattle were imported from the
365 U.S into Australia (54), supporting our phylodynamic finding that the common ancestral link
366 between *S*. Dublin isolates from North America and Australia emerged in the early-mid 20th
367 century. Following region-specific introductions, subsequent local antimicrobial and
368 husbandry practices may have contributed to the local evolution of *S.* Dublin (50,55).
369
370 Of note, among *S.* Dublin isolates from Australia, genomic analysis (cf. serotyping) revealed a
371 smaller population of ST74 isolates. *S.* Dublin ST74 was previously identified as *S*. Enteritidis
372 ST74, and sits as an intermediate between *S*. Dublin and *S*. Enteritidis (20), and has been
373 understudied to date in studies of *S.* Dublin. The difference between the antigenic formula of
374 *S*. Dublin and *S*. Enteritidis is in the H1 flagella region, which is typed as "*g,p*" for *S.* Dublin
375 and "*g,m*" for *S.* Enteritidis. ST74 *S.* Dublin genomes were characterised by: (i) a lack of any
376 AMR or HMR determinants; (ii) lack of complete SPI-6 regions, specifically the T6SS, and
377 (iii) a lack of putative virulence determinants including ST313-gi, Gifsy-2 like prophage and
378 SPI-19, which encodes a T6SS mechanism for intestinal colonisation and survival that interacts
379 with the host by mediating macrophage cytotoxicity (55).
380
381 The lack of the Vi antigen in 1,302/1,303 (99.9%) *S*. Dublin genomes has several implications.
382 First, the antigenic formula of *S*. Dublin, 1,9,12[Vi] may need to be reviewed if most *S.* Dublin
383 genomes lack the machinery to express the Vi capsule. These limitations with serotyping have
384 been highlighted in a previous study, which suggested a transition to a novel genotyping
385 scheme that would prevent these phenotypic discrepancies (56). Second, the Vi antigen is a
386 vaccine target for *S.* Typhi (57), and the Vi antigen has been explored as a target for *S.* Dublin
387 (58). While previous studies have noted that some *S.* Dublin genomes may be capable of
388 producing the Vi antigen (58), the genomic data from this study shows that these genomes are

389 in the minority of the *S.* Dublin population and may not be stable targets for *S.* Dublin specific
390 vaccines.
391
392 Our phenotypic data demonstrated a striking difference in replication dynamics between ST10
393 and ST74 populations in human macrophages. ST74 isolates replicated significantly over 24
394 hours, whereas ST10 isolates were rapidly cleared after 9 hours of infection. ST74 induced
395 significantly less host cell death during the early-mid stage of macrophage infection, supported
396 by limited processing and release of IL-1ß at 9 hpi. While NTS are generally potent
397 inflammasome activators (60), most supporting data come from laboratory-adapted *S.*
398 Typhimurium strains. Our findings suggest that ST74 isolates may employ immune evasion
399 mechanisms to avoid host recognition and activation of cell death signaling in early infection
400 stages. Similar trends have been observed with *S.* Typhimurium ST313, which induces less
401 inflammasome activation than ST19 during murine macrophage infection (61). This could
402 facilitate increased replication and dissemination at later stages of infection. Consistent with
403 this, we observed comparable cytotoxicity between ST10 and ST74 isolates at 24 hpi,
404 suggesting ST74 induces cell death via alternative mechanisms once intracellular bacterial
405 numbers are unsustainable. Further research is needed to identify genomic factors underpinning
406 these observations.
407
408 Although our machine learning approach predicted lower invasiveness for ST74 compared to
409 ST10, the increased genomic complexity of ST74 may support higher replication in
410 macrophages. We speculate that increased intracellular replication could enhance systemic
411 dissemination, though this requires *in vivo* validation. Invasiveness of *S. enterica* is often linked
412 to genome degradation (4,62–64). However, this is mostly based on studies of human-adapted
413 iNTS (ST313) and *S.* Typhi, leaving open the possibility that the additional genomic richness

414 of ST74 supports survival in diverse host species. An uncharacterised virulence factor may
415 underlie this replication advantage. Collectively, these findings highlight phenotypic
416 differences between *S*. Dublin populations ST10 and ST74. Enhanced intra-macrophage
417 survival of ST74 could promote invasive disease, whereas the prevalence of ST10 may relate
418 to better intestinal adaptation and enhanced faecal shedding. *In vivo* models are requireed to
419 test this hypothesis. Interestingly, the absence of SPI-19 in ST74, which encodes a T6SS, may
420 reflect adaptation to enhanced replication in macrophages. SPI-19 has been linked to intestinal
421 colonisation in poultry (23,56) and mucosal virulence in mice (56). It is possible that the
422 efficient replication of ST74 in macrophages may compensate for the absence of SPI-19,
423 relying instead on phagocyte uptake via M cells or dendritic cells. The complex pangenome of
424 ST74 compared to ST10 could further enhance survival within hosts. These findings highlight
425 important knowledge gaps in zoonotic NTS host-pathogen interactions and drivers of emerging
426 invasive NTS lineages with broad host ranges.
427
428 This study has limitations, including a focus on ST10 isolates from clade 1, which do not
429 represent global phylogenetic diversity. Nonetheless, our pangenome analysis identified >900
430 uncharacterised genes unique to ST74 , offering potential targets for future research. Another
431 limitation is the geographic bias in available genomes, with underrepresentation from Asia and
432 South America. This reflects broader disparities in genomic epidemiological studies but may
433 improve as public health genomics capacity expands globally.
434
435 Overall, this study represents the most comprehensive genomic study of *S.* Dublin to date,
436 systematically characterising antimicrobial, heavy metal and biocide resistance determinants,
437 in addition to exploring the virulome in the global population of *S.* Dublin. Importantly, our
438 phenotypic data reveals the caution required when making generalised statements about

439 infection outcomes and virulence mechanisms of *Salmonella* serovars. Our data clearly shows
440 that within the Dublin serovar, there are distinct phenotypic differences observed across
441 sequence types and host cell types, all of which could impact significantly on future
442 development of effective therapeutics or vaccine strategies for NTS infections. While the data
443 did not indicate an increasing trend of iNTS associated with *S*. Dublin, the potential public
444 health risk of this invasive pathogen suggests it may still warrant considering it a notifiable
445 disease, similar to typhoid and paratyphoid fever.
446
447 **METHODS**
448
449 ***Setting and dataset***
450 For Australian isolates, whole genome sequencing (WGS) was performed on all viable *S*.
451 Dublin isolates from human clinical samples received at the Microbiological Diagnostic Unit
452 Public Health Laboratory (MDU PHL), the primary bacterial reference laboratory for the State
453 of Victoria in Australia. In total, 53 *S*. Dublin genomes between 2000-2019 were included. For
454 publicly available data, we included *S*. Dublin sequences that had associated metadata
455 (geographical origin and date of sample collection), providing a total of 1,250 publicly
456 available sequences. Data were collected in accordance with the Victorian Public Health and
457 Wellbeing Act 2008. Ethical approval was received from the University of Melbourne Human
458 Research Ethics Committee (study number 1954615.3).
459
460 ***Genome quality control, assembly and serovar prediction***
461 Genomes were assembled and quality controlled using the Nullarbor pipeline v2.0.20191013
462 (https://github.com/tseemann/nullarbor). Briefly, Skesa v2.4.0 (59) was used to assemble the
463 genomes before determining the sequence type (ST) using the multilocus sequence typing

464 (MLST) scheme '*senterica'* within mlst v2.19.0 (https://github.com/tseemann/mlst). Kraken
465 v1.1.1 (60) was then used to confirm the taxonomic classification. Snippy v4.6.0
466 (https://github.com/tseemann/snippy) with parameters set to a 0.90 variant rate proportion
467 against a minimum coverage of 10X mapped the reads against a well-studied reference
468 genome, *S*. Dublin CT_02021853 (NC_011205.1). To be included in subsequent analysis,
469 genomes had to pass the following quality control parameters: mapped to ≥ 80% of the
470 reference genome; had a ≥ 80% taxonomic sequence similarity to *S. enterica*; N50 >25000,
471 and <300 contigs. To verify that each genome was *S*. Dublin, all sequences were typed using
472 *Salmonella* in silico Typing Resource (SISTR) v1.1.1 (61). The electrophoretic type of each
473 isolate was determined using Antimicrobial Resistance Identification by Assembly (ARIBA)
474 v2.14.5 (62) against the reference Du 2 (Genbank accession: M84972.1). The draft genome
475 assemblies were annotated using Prokka v1.14.6 (63).
476
477 ***Core genome phylogenomic analysis***
478 Variant calls from snippy were used to construct a core genome single nucleotide
479 polymorphism (SNP) alignment using snippy-core v4.6.0
480 (https://github.com/tseemann/snippy). Phaster v2020-12-22 (64) was used to create a BED file
481 containing prophage regions. The option '—mask' in snippy-core was used to exclude the
482 identified prophage regions from the BED file. Recombination was assessed and filtered using
483 Gubbins v2.4.1 (65). Constant sites from the reference genome were obtained using the script
484 iqtree-calc_const_sites.sh (https://github.com/MDU-PHL/mdu-tools/blob/master/bin/iqtree-
485 calc_const_sites.sh). A maximum-likelihood (ML) phylogeny was inferred using IQ-TREE
486 v2.1.0 (66) with parameters set to a GTR+G4 nucleotide substitution model with constant sites
487 and ultrafast bootstrapping (67) to 1000 replicates. The resulting ML tree was then visualised
488 using *ggtree* v2.3.3 R package (68). Population clades were defined using rhierBAPS v1.1.3

489 (69) to one level on an alignment of 2,957 core SNPS of 1,295 isolates in the ST10 *S.* Dublin
490 lineage.
491
492 ***In silico prediction of resistance determinants and plasmid replicons***
493 To screen for quinolone point mutations and acquired AMR determinants, ARIBA and
494 AbriTAMR v0.2.2 (https://github.com/MDU-PHL/abritamr) were used, respectively. The
495 AMR database used for this study was the NCBI AMRFinderPlus database v2020-01-22.1.
496 Each isolate's susceptibility profile was classified as either susceptible; resistant to 1-2
497 antimicrobials, or multidrug resistant (MDR). Heavy metal and biocide determinants were
498 identified by screening the AMRFinder database v2020-07-16.2 with AMRFinder v3.8.4 (70).
499 Replicon types were determined using ABRicate v1.0.1 (https://github.com/tseemann/abricate)
500 at a threshold of 80% nucleotide identity and 95% coverage, and screening against the
501 Plasmidfinder database (71). A strict threshold was applied to ensure the detection of only
502 unambiguous replicon types. To establish the most common resistant profiles, co-occurrence
503 matrices of resistant determinants were constructed in R using *igraph* v1.2.4.1 (72).
504
505 ***Virulome analysis***
506 Virulence genes were identified using ABRicate at 90% nucleotide identity/coverage against
507 the virulence factor database (vfdb) v2018-03-18 (73). Databases from previous studies
508 (16,27,35,74–78) were also interrogated and collated. This included a database containing
509 additional virulent determinants and *Salmonella* pathogenicity islands (SPIs) previously
510 implicated with *S.* Dublin invasome (35,41). Using ABRicate, the presence of SPIs -1, -2, -6
511 and -19 were identified at 80% ID and 10% COV (Supplementary Table 14). ABRicate was
512 also used to screen the manually created SPI determinant database for genes relevant to SPI-1,
513 -2, -6 and -19 with a threshold of 90% identity/coverage (Supplementary Table 14). To quantify

514 invasiveness, index scores were calculated *in silico* for each isolate using Wheeler *et al.*'s tool
515 developed in 2018 for inferring the likelihood of invasiveness
516 (http://www.github.com/UCanCompBio/invasive_*Salmonella*), with a higher score for an
517 isolate deemed more invasive (38). Prior to running the tool, a set of reference genomes
518 consisting of invasive and non-invasive *Salmonella* serovars were used as a validation set
519 (Supplementary Table 8). The validation results were then visualised using *ggtree*.
520
521 ***Bayesian phylodynamic analysis***
522 A subset of 660 *S.* Dublin genomes from the main cluster was used for BEAST v1.10.4 (79)
523 analysis. This subset comprised all Australian genomes and a proportion of international *S.*
524 Dublin genomes. The sampling strategy for selecting representative international genomes
525 involved capturing all geographical regions and sources harbouring distinct susceptibility
526 profiles. When two genomes demonstrated the same AMR profile and were from the same
527 region and source, the oldest genome was preferred. Recombination sites were filtered using
528 Gubbins. A core genome SNP alignment of these genomes was created using snippy-core
529 v4.6.0 and then a ML phylogeny was inferred as above. Temporal signal was assessed using
530 TempEst v1.5.3 (80) by assessing the best-fitting root using the heuristic residual mean squared
531 method, with an R^2 of 0.31. The core alignment was then used to create an xml file in BEAUti
532 v1.10.4 using the GTR+G4 substitution model. To identify the most appropriate model for our
533 dataset, a combination of using either a "relaxed lognormal" or a "strict" molecular clock with
534 either a "coalescent constant" or a "coalescent exponential" population prior was tested. For
535 all models, the Markov chain Monte Carlo chain length was set to 300,000,000 and sampling
536 was set to every 20,000 trees with the marginal likelihood estimation set to "generalised
537 stepping stone (GSS)" to assess the statistical support for models and evaluate the best-fit
538 model. The analysis was repeated in triplicates with and without tip dates to ensure there was

539 no temporal bias. Bayesian evaluation of temporal signal (BETS) was used to determine
540 whether a temporal signal was present (81). To optimise computational resource and time,
541 BEAST v1.10.4 was used with BEAGLE v3.0.2 (82). A Maximum Clade Credibility (MCC)
542 tree from the highest supported model using GSS was extracted using TreeAnnotator v1.10.4
543 and median heights. The resulting MCC tree was then visualised using *ggtree*.
544
545 ***Long read sequencing***
546 The Oxford Nanopore Technologies MinION platform was used to obtain complete genomes
547 of six Australian *S*. Dublin genomes (Supplementary Table 13). These genomes, comprised of
548 ST10 lineage clade 1 (AUSMDU00056868 and AUSMDU00035676,) and ST74
549 (AUSMDU00016676 and AUSMDU00021231), were selected based on their AMR profile,
550 virulome and index scores. To prepare new DNA libraries for long read sequencing, genomes
551 were freshly re-cultured. DNA was extracted using the Virus/Pathogen DSP midi kit on the
552 QiaSymphony SP instrument. Sequencing libraries were prepared using a Ligation sequencing
553 kit (SQK-LSK109) with native barcode expansion and sequenced for 48 hours on a GridION
554 Mk2 instrument using a R9.4 flowcell. WGS was performed using the Illumina NextSeq
555 500/550 platform (Illumina, San Diego, CA). Demultiplexed long reads and corresponding
556 WGS reads were subjected to QC to exclude unreliable reads using fastp v0.20.1 (83) and
557 Filtlong v0.2.1 (https://github.com/rrwick/Filtlong), respectively. Long reads were assembled
558 using Trycycler v0.4.1 (84). The final sequence was polished using Medaka v1.4.3
559 (https://github.com/nanoporetech/medaka). To ensure small plasmids were not excluded during
560 the initial QC step, hybrid assemblies using both long and WGS reads were generated
561 Unicycler v0.4.4 (85). Trycycler assemblies were checked against Unicycler assemblies with
562 Bandage v0.8.1 (86). The final genome assemblies were confirmed as *S*. Dublin using SISTR
563 and annotated using both Prokka v1.14.6 (63) for consistency with the draft genome assemblies

564 and Bakta v1.10.1 (87) which provides for more detailed annotations (Supplementary Table
565 13). Both Prokka and Bakta annotations were in agreement for AMR, HMR and virulence
566 genes, with Bakta annotating between 3-7 additional coding sequences (CDS) which were
567 largely 'hypothetical protein'.
568
569 Chromosomal assemblies were aligned to complete genomes of known *S*. Dublin references
570 CT_02021853 (CP001144.1, without Vi capsule) and CFSAN000518 (CP074226.1, with Vi
571 capsule) and visualised using Blast Ring Image Generator (BRIG) v0.95 (88). Plasmid
572 assemblies were screened against the PlasmidFinder database (71) and mob-typer v3.1.0 (89)
573 to identify replicon and relaxase types, respectively. Plasmid profiles were subjected to
574 BLASTn against previously identified IncX1/IncFII(S) virulence plasmids reported in *S.*
575 Dublin and IncN plasmids associated with serovars of *Salmonella* (Supplementary Table 5).
576 Genome comparisons of plasmids demonstrating the top four highest BLASTn max scores
577 were visualised using BRIG. Bakta, PlasmidFinder and ISFinder (90) were used to annotate
578 the regions of interest, while Easyfig v2.2.2 (91) was used to compare regions of the genome.
579 Regions of the genome were visualised using the R package *gggenomes* v0.9.12.9000
580 (https://github.com/thackl/gggenomes).
581
582 ***Human cell line infections***
583 Human macrophage (THP-1) (ATCC® TIB-202™) and colonic epithelial (HT-29) (ATCC®
584 HTB-38™) cell lines were maintained in Roswell Park Memorial Institute (RPMI) 1640 media
585 + 200 mM GlutaMAX (Life Technologies) supplemented with 10% v/v Fetal Bovine Serum
586 (FBS; Bovogen) and grown in a humidified 5% CO2 37ºC incubator. THP-1 monocytes were
587 differentiated into macrophages with 50 ng/mL phorbol 12-myristiate-12 acetate (PMA,
588 Sigma-Aldrich) for 72 hours prior to infection.

589

590 Single colonies of each *S*. Dublin isolate were inoculated into 10 mL Luria Bertani (LB) broth
591 and grown overnight at 37ºC at 200 rpm, then sub-cultured for 3 hours in the same conditions
592 in 5 mL LB. Colony forming units/mL were measured by absorbance at 600 nM (OD_{600}). THP-
593 1 and HT-29 cells were infected at a multiplicity of infection (MOI) of 10 in RPMI in triplicate
594 wells of a 96-well plate and centrifuged at 525 x g for 5 minutes to synchronize bacterial
595 uptake. Infected cells were incubated at 37ºC for 30 minutes, then infective media removed
596 and replaced with 100 µg/mL gentamicin in 10% v/v FBS/RPMI to inhibit extracellular
597 bacterial growth. 0 hours post infection (hpi) samples were collected at this time to measure
598 initial bacterial uptake. Cells were then incubated in high dose gentamicin for 1 hour, then
599 replaced with 10 µg/mL gentamicin in 10% v/v FBS/RPMI for the remainder of the infection.
600 For THP-1 cells, samples were collected at time 0-, 3-, 9- and 24-hours post-infection. For HT-
601 29 cells, samples were collected at 0- and 24-hours post-infection.

602

603 Cytotoxicity of infection was measured by lactate dehydrogenase (LDH) release by infected
604 cells before lysis for intracellular bacterial enumeration. Briefly, 35 uL of infected (and
605 uninfected) cell culture supernatants were collected from each well and LDH quantified as per
606 manufacturer's instructions (Promega), with percent cytotoxicity calculated as a proportion of
607 lysed control cells and blank media. Following this, infected cells were washed three times
608 with warm phosphate-buffered saline (PBS) to remove any lingering extracellular bacteria,
609 then lysed in 0.1% Triton X-100/PBS and plated out onto LB agar after serial dilution. Bacterial
610 enumeration and cell viability assays were performed over 3 biological replicates, each
611 performed independently, with a new passage of host cells, on a separate day. Within each
612 biological replicate, technical triplicates were performed for each isolate. All statistical
613 analyses were performed using Prism software (GraphPad Software v9.0) and determined by

614 nested students t-test, which allowed for inclusion of individual isolates in sub-groups of each
615 sequence type (ST10 vs ST74).
616
617 ***Measurement of cellular responses***
618 THP-1 cells were infected at an MOI of 10 with a representative isolate from each of the ST10
619 and ST74 lineages as described above, then lysed in radio-immunoprecipitation (RIPA) buffer
620 (20 mM Tris pH 8.0, 0.5 mM EDTA, 150 mM NaCl, 1% v/v Triton X-100, 0.5% w/v sodium
621 deoxycholate, 0.1% w/v SDS) supplemented with Complete protease and phosphatase inhibitor
622 cocktails (Roche) at 0-, 3-, 8- and 24 hpi. Total protein concentration was quantified by
623 Bicinchoninic acid (BCA) assay and 15 µg separated on 4-12% Bolt Bis-Tris polyacrylamide
624 gels (Thermo Scientific), transferred to nitrocellulose (iBlot, Thermo Scientific) and blotted
625 for cleaved IL-1β (clone D3A3Z, Cell Signalling). Cell culture supernatants were also collected
626 from 96-well plate infections at 9 hpi and secreted IL-1β measured by DuoSet© Human IL-
627 1β/IL-1F2 ELISA as per manufacturer's instructions (R&D Systems). A core genome SNP ML
628 phylogeny was constructed on the Australian ST10 lineage to demonstrate the genetic
629 relationship of representative ST10 isolates that underwent *in vitro* phenotypic assays.
630
631 ***Pangenome analysis***
632 The pangenomes of the isolates used in the macrophages and epithelial infections were
633 analysed using Panaroo v1.3.4 (92) set to default threshold settings, under strict mode and with
634 the removal of invalid genes on the Prokka annotated draft genome assemblies (Supplementary
635 Table 11). A SNP distance matrix was generated using snps-dist v0.8.2
636 (https://github.com/tseemann/snp-dists) based on the core genome alignment of these isolates,
637 which had been previously used to construct a maximum likelihood (ML) tree.
638

DATA AVAILABILITY

Paired end reads of public data were obtained from either the European Nucleotide Archive (ENA) or National Center for Biotechnology Information (NCBI). The Australian short read data and complete genomes for the four Australian *S.* Dublin isolates are available at the NCBI Sequence Read Archive under BioProject PRJNA319593. Details of all 1,303 genomes included in the study are available in Supplementary Tables 1-14. These supplementary tables also includes *i*) the resistance, virulence, Vi and *fliC* profiles of all 1,303 genomes; *ii*) the genbank accession numbers of all reference genomes, virulence determinants and IncN plasmids used in this study, *iii*) genomic annotations of putative novel plasmids, and *iv*) all raw CFU, cytotoxicity and ELISA values from the phenotypic analyses. The interactive tree is available in Microreact under https://microreact.org/project/sdublinpaper).

CODE AVAILABILITY

The machine learning tool developed by Wheeler *et al*. for predicting the likelihood of invasiveness is available in a public Github depository http://www.github.com/UCanCompBio/invasive_*Salmonella*.

REFERENCES

1. Stanaway JD, Parisi A, Sarkar K, Blacker BF, Reiner RC, Hay SI, et al. The Global Burden of Non-typhoidal *Salmonella* Invasive Disease: A Systematic Analysis for the Global Burden of Disease Study 2017. The Lancet Infectious Diseases. 2019;19(12):1312–24.

2. Parisi A, Crump JA, Stafford R, Glass K, Howden BP, Kirk MD. Increasing incidence of invasive nontyphoidal *Salmonella* infections in Queensland, Australia, 2007-2016. PLOS Neglected Tropical Diseases. 2019 Mar 18;13(3):e0007187.

3. Mughini-Gras L, Pijnacker R, Duijster J, Heck M, Wit B, Veldman K, et al. Changing Epidemiology of Invasive Non-typhoid *Salmonella* Infection: A Nationwide Population-based Registry Study. Clinical Microbiology and Infection. 2020;26(7):941.e9-941.e14.

4. Kingsley RA, Msefula CL, Thomson NR, Kariuki S, Holt KE, Gordon MA, et al. Epidemic Multiple Drug Resistant *Salmonella* Typhimurium Causing Invasive Disease in Sub-Saharan Africa have a Distinct Genotype. Genome Res. 2009;19(12):2279–87.

5. Cheng RA, Eade CR, Wiedmann M. Embracing Diversity: Differences in Virulence Mechanisms, Disease Severity, and Host Adaptations Contribute to the Success of Nontyphoidal *Salmonella* as a Foodborne Pathogen. Front Microbiol. 2019 Jun 26;10:1368.

6. Williamson DA, Lane CR, Easton M, Valcanis M, Strachan J, Veitch MG, et al. Increasing Antimicrobial Resistance in Nontyphoidal *Salmonella* Isolates in Australia from 1979 to 2015. Antimicrob Agents Chemother. 2018;62(2). Available from: https://www.ncbi.nlm.nih.gov/pmc/articles/PMC5786757/

7. Mangat CS, Bekal S, Avery BP, Côté G, Daignault D, Doualla-Bell F, et al. Genomic Investigation of the Emergence of Invasive Multidrug-Resistant *Salmonella enterica* Serovar Dublin in Humans and Animals in Canada. Antimicrobial Agents and Chemotherapy. 2019;63(6).

8. Reichel MP, Wahl LC, Hill FI. Review of Diagnostic Procedures and Approaches to Infectious Causes of Reproductive Failures of Cattle in Australia and New Zealand. Front Vet Sci. 2018 Oct 2;5.

9. Kirchner M, McLaren I, Clifton-Hadley FA, Liebana E, Wales AD, Davies RH. A Comparison Between Longitudinal Shedding Patterns of *Salmonella* Typhimurium and *Salmonella* Dublin on Dairy Farms. Veterinary Record. 2012 Aug 25;171(8):194–194.

10. McDonough PL, Fogelman D, Shin SJ, Brunner MA, Lein DH. *Salmonella enterica* Serotype Dublin Infection: an Emerging Infectious Disease for the Northeastern United States. J Clin Microbiol. 1999 Aug;37(8):2418–27.

11. Davidson KE, Byrne BA, Pires AFA, Magdesian KG, Pereira RV. Antimicrobial resistance trends in fecal *Salmonella* isolates from northern California dairy cattle admitted to a veterinary teaching hospital, 2002-2016. PLoS One. 2018;13(6). Available from: https://www.ncbi.nlm.nih.gov/pmc/articles/PMC6023112/

12. Fenske GJ, Thachil A, McDonough PL, Glaser A, Scaria J. Geography Shapes the Population Genomics of *Salmonella enterica* Dublin. Genome Biol Evol. 2019 Aug 1;11(8):2220–31.

13. Sia CM, Baines SL, Valcanis M, Lee DYJ, Gonçalves da Silva A, Ballard SA, et al. Genomic Diversity of Antimicrobial Resistance in Non-typhoidal *Salmonella* in Victoria, Australia. Microbial Genomics. 2021;7(12):000725.

14. Paudyal N, Pan H, Elbediwi M, Zhou X, Peng X, Li X, et al. Characterization of *Salmonella* Dublin isolated from bovine and human hosts. BMC Microbiology. 2019 Oct 16;19(1):226.

15. Harvey RR, Friedman CR, Crim SM, Judd M, Barrett KA, Tolar B, et al. Epidemiology of *Salmonella enterica* Serotype Dublin Infections among Humans, United States, 1968–2013 - Volume 23, Number 9—September 2017 - Emerging Infectious Diseases journal - CDC. [cited 2020 Nov 24]; Available from: https://wwwnc.cdc.gov/eid/article/23/9/17-0136_article

16. Hsu CH, Li C, Hoffmann M, McDermott P, Abbott J, Ayers S, et al. Comparative Genomic Analysis of Virulence, Antimicrobial Resistance, and Plasmid Profiles of

711 *Salmonella* Dublin Isolated from Sick Cattle, Retail Beef, and Humans in the United
712 States. Microbial Drug Resistance. 2019 May 31;25(8):1238–49.

713 17. Magiorakos AP, Srinivasan A, Carey RB, Carmeli Y, Falagas ME, Giske CG, et al.
714 Multidrug-Resistant, Extensively Drug-resistant and Pandrug-resistant Bacteria: An
715 International Expert Proposal for Interim Standard Definitions for Acquired Resistance.
716 Clinical Microbiology and Infection. 2012;18(3):268–81.

717 18. Mangat CS, Bekal S, Irwin RJ, Mulvey MR. A Novel Hybrid Plasmid Carrying Multiple
718 Antimicrobial Resistance and Virulence Genes in *Salmonella enterica* Serovar Dublin.
719 Antimicrob Agents Chemother. 2017 May 24;61(6):e02601-16.

720 19. Langridge GC, Fookes M, Connor TR, Feltwell T, Feasey N, Parsons BN, et al. Patterns
721 of Genome Evolution that have Accompanied Host Adaptation in *Salmonella*. Proc Natl
722 Acad Sci USA. 2015;112(3):863–8.

723 20. Achtman M, Wain J, Weill FX, Nair S, Zhou Z, Sangal V, et al. Multilocus Sequence
724 Typing as a Replacement for Serotyping in *Salmonella enterica*. PLoS Pathogens.
725 2012;8(6):e1002776.

726 21. Selander RK, Smith NH, Li J, Beltran P, Ferris KE, Kopecko DJ, et al. Molecular
727 Evolutionary Genetics of the Cattle-Adapted Serovar *Salmonella* Dublin. J Bacteriol.
728 1992;174(11):3587–92.

729 22. Pezoa D, Blondel CJ, Silva CA, Yang HJ, Andrews-Polymenis H, Santiviago CA, et al.
730 Only One of the Two Type VI Secretion Systems Encoded in the *Salmonella enterica*
731 Serotype Dublin Genome is Involved in Colonization of the Avian and Murine Hosts.
732 Veterinary Research. 2014;45(1):2.

733 23. Blondel CJ, Jiménez JC, Contreras I, Santiviago CA. Comparative Genomic Analysis
734 Uncovers 3 Novel Loci Encoding Type Six Secretion Systems Differentially Distributed
735 in *Salmonella* Serotypes. BMC Genomics. 2009 Aug 4;10:354.

736 24. Blondel CJ, Amaya FA, Bustamante P, Santiviago CA, Pezoa D. Identification and
737 distribution of new candidate T6SS effectors encoded in *Salmonella* Pathogenicity Island
738 6. Front Microbiol. 2023;14. Available from:
739 https://www.frontiersin.org/journals/microbiology/articles/10.3389/fmicb.2023.1252344/f
740 ull

741 25. Amaya FA, Blondel CJ, Barros-Infante MF, Rivera D, Moreno-Switt AI, Santiviago CA,
742 et al. Identification of Type VI Secretion Systems Effector Proteins That Contribute to
743 Interbacterial Competition in *Salmonella* Dublin. Frontiers in Microbiology. 2022;13.
744 Available from: https://www.frontiersin.org/article/10.3389/fmicb.2022.811932

745 26. Vilela FP, Gomes CN, Paziani MH, Braz VS, Rodrigues D dos P, Costa RG, et al.
746 Virulence traits and expression of *bstA, fliC* and *sopE2* in *Salmonella* Dublin strains
747 isolated from humans and animals in Brazil. Infection, Genetics and Evolution.
748 2020;80:104193.

749 27. Hammarlöf DL, Kröger C, Owen SV, Canals R, Lacharme-Lora L, Wenner N, et al. Role
750 of a Single Noncoding Nucleotide in the Evolution of an Epidemic African Clade of
751 *Salmonella*. Proc Natl Acad Sci U S A. 2018;115(11):E2614–23.

752 28. Herrero-Fresno A, Espinel IC, Spiegelhauer MR, Guerra PR, Andersen KW, Olsen JE.
753 The Homolog of the Gene *bstA* of the BTP1 Phage from *Salmonella enterica* Serovar
754 Typhimurium ST313 Is an Antivirulence Gene in *Salmonella enterica* Serovar Dublin.
755 Infection and Immunity. 2018;86(1).

756 29. Mohammed M, Cormican M. Whole Genome Sequencing Provides Insights into the
757 Genetic Determinants of Invasiveness in *Salmonella* Dublin. Epidemiology and Infection.
758 2016;144(11):2430–9.

759 30. De Sousa Violante M, Podeur G, Michel V, Guillier L, Radomski N, Lailler R, et al. A
760 Retrospective and Regional Approach Assessing the Genomic Diversity of *Salmonella*
761 Dublin. NAR Genom Bioinform. 2022 Jul 9;4(3):lqac047.

762 31. Ingle DJ, Ambrose RL, Baines SL, Duchene S, Gonçalves da Silva A, Lee DYJ, et al.
763 Evolutionary Dynamics of Multidrug Resistant *Salmonella enterica* serovar 4,[5],12:i:- in
764 Australia. Nature Communications. 2021;12(1):4786.

765 32. Duchêne S, Holt KE, Weill FX, Le Hello S, Hawkey J, Edwards DJ, et al. Genome-scale
766 Rates of Evolutionary Change in Bacteria. Microb Genom. 2016 Nov 30;2(11):e000094.

767 33. Silva C, Puente JL, Calva E. *Salmonella* Virulence Plasmid: Pathogenesis and Ecology.
768 Pathogens and Disease. 2017;75(6).

769 34. Harmer CJ, Hall RM. IS26 Family Members IS257 and IS1216 Also Form Cointegrates
770 by Copy-In and Targeted Conservative Routes. mSphere. 2020;5(1):811.

771 35. Mohammed M, Le Hello S, Leekitcharoenphon P, Hendriksen R. The invasome of
772 *Salmonella* Dublin as revealed by whole genome sequencing. BMC Infect Dis. 2017 Aug
773 4;17. Available from: https://www.ncbi.nlm.nih.gov/pmc/articles/PMC5544996/

774 36. Hong SF, Chiu CH, Chu C, Feng Y, Ou JT. Complete Nucleotide Sequence of a Virulence
775 Plasmid of *Salmonella enterica* Serovar Dublin and Its Phylogenetic Relationship to the
776 Virulence Plasmids of Serovars Choleraesuis, Enteritidis and Typhimurium. FEMS
777 Microbiology Letters. 2008;282(1):39–43.

778 37. Chu C, Feng Y, Chien AC, Hu S, Chu CH, Chiu CH. Evolution of Genes on the
779 *Salmonella* Virulence Plasmid Phylogeny Revealed From Sequencing of the Virulence
780 Plasmids of *S. enterica* Serotype Dublin and Comparative Analysis. Genomics.
781 2008;92(5):339–43.

782 38. Wheeler NE, Gardner PP, Barquist L. Machine Learning Identifies Signatures of Host
783 Adaptation in the Bacterial Pathogen *Salmonella enterica*. PLoS Genetics.
784 2018;14(5):e1007333.

785 39. Lambert MA, Smith SG. The PagN protein of *Salmonella enterica* Serovar Typhimurium
786 is an Adhesin and Invasin. BMC Microbiology. 2008;8(1):142.

787 40. Folkesson A, Advani A, Sukupolvi S, Pfeifer JD, Normark S, Löfdahl S. Multiple
788 Insertions of Fimbrial Operons Correlate with the Evolution of *Salmonella* Serovars
789 Responsible for Human Disease. Molecular Microbiology. 1999;33(3):612–22.

41. Herrero-Fresno A, Wallrodt I, Leekitcharoenphon P, Olsen JE, Aarestrup FM, Hendriksen RS. The Role of the *st313-td* Gene in Virulence of *Salmonella* Typhimurium ST313. PLOS ONE. 2014 Jan 3;9(1):e84566.

42. Sabbagh SC, Forest CG, Lepage C, Leclerc JM, Daigle F. So Similar, Yet So Different: Uncovering Distinctive Features in the Genomes of *Salmonella enterica* Serovars Typhimurium and Typhi. FEMS Microbiology Letters. 2010;305(1):1–13.

43. Chen LM, Kaniga K, Galán JE. *Salmonella* spp. are cytotoxic for cultured macrophages. Molecular Microbiology. 1996;21(5):1101–15.

44. Miao EA, Mao DP, Yudkovsky N, Bonneau R, Lorang CG, Warren SE, et al. Innate immune detection of the type III secretion apparatus through the NLRC4 inflammasome. Proceedings of the National Academy of Sciences. 2010 Feb 16;107(7):3076–80.

45. Bergsbaken T, Fink SL, Cookson BT. Pyroptosis: host cell death and inflammation. Nat Rev Microbiol. 2009 Feb;7(2):99–109.

46. Doerflinger M, Deng Y, Whitney P, Salvamoser R, Engel S, Kueh AJ, et al. Flexible Usage and Interconnectivity of Diverse Cell Death Pathways Protect against Intracellular Infection. Immunity. 2020 Sep;53(3):533-547.e7.

47. Kudirkiene E, Sørensen G, Torpdahl M, de Knegt LV, Nielsen LR, Rattenborg E, et al. Epidemiology of *Salmonella enterica* Serovar Dublin in Cattle and Humans in Denmark, 1996 to 2016: a Retrospective Whole-Genome-Based Study. Applied and Environmental Microbiology. 2020;86(3):1.

48. Cheng G, Ning J, Ahmed S, Huang J, Ullah R, An B, et al. Selection and Dissemination of Antimicrobial Resistance in Agri-food Production. Antimicrob Resist Infect Control. 2019;8:158.

49. Srednik ME, Lantz K, Hicks JA, Morningstar-Shaw BR, Mackie TA, Schlater LK. Antimicrobial Resistance and Genomic Characterization of *Salmonella* Dublin Isolates in Cattle from the United States. PLOS ONE. 2021 Sep 21;16(9):e0249617.

50. Fritz HM, Pereira RV, Toohey-Kurth K, Marshall E, Tucker J, Clothier KA. *Salmonella enterica* Serovar Dublin from Cattle in California from 1993–2019: Antimicrobial Resistance Trends of Clinical Relevance. Antibiotics (Basel). 2022;11(8):1110.

51. McMillan EA, Jackson CR, Frye JG. Transferable Plasmids of *Salmonella enterica* Associated With Antibiotic Resistance Genes. Frontiers in Microbiology. 2020;11. Available from: https://www.frontiersin.org/article/10.3389/fmicb.2020.562181

52. Zhang Y, Lei CW, Chen X, Yao TG, Yu JW, Hu WL, et al. Characterization of IncC Plasmids in Enterobacterales of Food-Producing Animals Originating From China. Front Microbiol. 2020;11:580960.

53. Izzo M, Mohler V, House J. Antimicrobial Susceptibility of *Salmonella* Isolates Recovered From Calves with Diarrhoea in Australia. Australian Veterinary Journal. 2011;89(10):402–8.

54. O'Connell J. Australian Food Timeline. 1930 [cited 2022 Nov 11]. Australian food history timeline - Brahman cattle imported. Available from: https://australianfoodtimeline.com.au/brahman-cattle-imported/

55. Schroll C, Huang K, Ahmed S, Kristensen BM, Pors SE, Jelsbak L, et al. The SPI-19 encoded type-six secretion-systems (T6SS) of *Salmonella enterica* serovars Gallinarum and Dublin play different roles during infection. Veterinary Microbiology. 2019;230:23–31.

56. Chattaway MA, Langridge GC, Wain J. *Salmonella* Nomenclature in the Genomic Era: A Time for Change. Sci Rep. 2021;11(1):7494.

57. Hu X, Chen Z, Xiong K, Wang J, Rao X, Cong Y. Vi Capsular Polysaccharide: Synthesis, Virulence, and Application. Critical Reviews in Microbiology. 2017;43(4):440–52.

58. Janis C, Grant AJ, McKinley TJ, Morgan FJE, John VF, Houghton J, et al. *In Vivo* Regulation of the Vi Antigen in *Salmonella* and Induction of Immune Responses with an *in vivo*-inducible Promoter. Infect Immun. 2011;79(6):2481–8.

59. Souvorov A, Agarwala R, Lipman DJ. SKESA: Strategic K-mer Extension for Scrupulous Assemblies. Genome Biology. 2018;19(1):153.

60. Wood DE, Salzberg SL. Kraken: ultrafast metagenomic sequence classification using exact alignments. Genome Biology. 2014 Mar 3;15(3):R46.

61. Yoshida CE, Kruczkiewicz P, Laing CR, Lingohr EJ, Gannon VPJ, Nash JHE, et al. The *Salmonella In Silico* Typing Resource (SISTR): An Open Web-accessible Tool for Rapidly Typing and Subtyping Draft *Salmonella* Genome Assemblies. PLoS One. 2016;11(1):e0147101.

62. Hunt M, Mather AE, Sánchez-Busó L, Page AJ, Parkhill J, Keane JA, et al. ARIBA: Rapid Antimicrobial Resistance Genotyping Directly from Sequencing Reads. Microb Genom. 2017;3(10). Available from: https://www.ncbi.nlm.nih.gov/pmc/articles/PMC5695208/

63. Seemann T. Prokka: Rapid Prokaryotic Genome Annotation. Bioinformatics (Oxford, England). 2014;30(14):2068–9.

64. Arndt D, Grant JR, Marcu A, Sajed T, Pon A, Liang Y, et al. PHASTER: a better, faster version of the PHAST phage search tool. Nucleic Acids Res. 2016 Jul 8;44(Web Server issue):W16–21.

65. Croucher NJ, Page AJ, Connor TR, Delaney AJ, Keane JA, Bentley SD, et al. Rapid Phylogenetic Analysis of Large Samples of Recombinant Bacterial Whole Genome Sequences Using Gubbins. Nucleic Acids Research. 2015;43(3):e15.

66. Nguyen LT, Schmidt HA, von Haeseler A, Minh BQ. IQ-TREE: A Fast and Effective Stochastic Algorithm for Estimating Maximum-Likelihood Phylogenies. Mol Biol Evol. 2015 Jan 1;32(1):268–74.

67. Minh BQ, Nguyen MAT, von Haeseler A. Ultrafast Approximation for Phylogenetic Bootstrap. Mol Biol Evol. 2013 May 1;30(5):1188–95.

867 68. Yu G, Smith DK, Zhu H, Guan Y, Lam TTY. *ggtree*: An R Package for Visualization and
868 Annotation of Phylogenetic Trees with their Covariates and other Associated Data.
869 Methods in Ecology and Evolution. 2017;8(1):28–36.

870 69. Tonkin-Hill G, Lees JA, Bentley SD, Frost SDW, Corander J. RhierBAPS: An R
871 Implementation of the Population Clustering Algorithm hierBAPS. Wellcome Open Res.
872 2018;3:93.

873 70. Feldgarden M, Brover V, Haft DH, Prasad AB, Slotta DJ, Tolstoy I, et al. Using the NCBI
874 AMRFinder Tool to Determine Antimicrobial Resistance Genotype-Phenotype
875 Correlations Within a Collection of NARMS Isolates. bioRxiv. 2019;550707.

876 71. Carattoli A, Zankari E, García-Fernández A, Larsen MV, Lund O, Villa L, et al. *In Silico*
877 Detection and Typing of Plasmids using PlasmidFinder and Plasmid Multilocus Sequence
878 Typing. Antimicrobial Agents and Chemotherapy. 2014 Jul 1;58(7):3895–903.

879 72. Csardi G, Nepusz T. The igraph software package for complex network research.
880 InterJournal Complex Systems. 2006;1695(Journal Article).

881 73. Chen L, Zheng D, Liu B, Yang J, Jin Q. VFDB 2016: Hierarchical and Refined Dataset
882 for Big Data Analysis—10 Years On. Nucleic Acids Res. 2016;44:D694–7.

883 74. Mansour MN, Yaghi J, El Khoury A, Felten A, Mistou MY, Atoui A, et al. Prediction of
884 *Salmonella* Serovars Isolated from Clinical and Food Matrices in Lebanon and Genomic-
885 based Investigation Focusing on Enteritidis Serovar. International Journal of Food
886 Microbiology. 2020;333:108831.

887 75. Suez J, Porwollik S, Dagan A, Marzel A, Schorr YI, Desai PT, et al. Virulence Gene
888 Profiling and Pathogenicity Characterization of Non-Typhoidal *Salmonella* Accounted for
889 Invasive Disease in Humans. PLoS One. 2013 Mar 7;8(3):e58449.

890 76. Sévellec Y, Vignaud ML, Granier SA, Lailler R, Feurer C, Le Hello S, et al. Polyphyletic
891 Nature of *Salmonella enterica* Serotype Derby and Lineage-Specific Host-Association
892 Revealed by Genome-Wide Analysis. Frontiers in Microbiology. 2018;9:891.

893 77. Hayward MR, Jansen VA, Woodward MJ. Comparative Genomics of *Salmonella enterica*
894 serovars Derby and Mbandaka, Two Prevalent Serovars Associated with Different
895 Livestock Species in the UK. BMC Genomics. 2013;14:365.

896 78. Kérouanton A, Hirchaud E, Rose V, Esnault E, Naquin D, Denis M. First Complete
897 Genome Sequence of a *Salmonella enterica* subsp. *enterica* Serovar Derby Strain
898 Associated with Pork in France. Genome Announc. 2015;3(4):e00853-15.

899 79. Suchard MA, Lemey P, Baele G, Ayres DL, Drummond AJ, Rambaut A. Bayesian
900 Phylogenetic and Phylodynamic Data Integration Using BEAST 1.10. Virus Evolution.
901 2018;4(1). Available from: https://doi.org/10.1093/ve/vey016

902 80. Rambaut A, Lam TT, Max Carvalho L, Pybus OG. Exploring the Temporal Structure of
903 Heterochronous Sequences using TempEst (formerly Path-O-Gen). Virus Evol.
904 2016;2(1):vew007.

81. Duchene S, Lemey P, Stadler T, Ho SYW, Duchene DA, Dhanasekaran V, et al. Bayesian Evaluation of Temporal Signal in Measurably Evolving Populations. Molecular Biology and Evolution. 2020;37(11):3363–79.

82. Ayres DL, Darling A, Zwickl DJ, Beerli P, Holder MT, Lewis PO, et al. BEAGLE: An Application Programming Interface and High-Performance Computing Library for Statistical Phylogenetics. Systematic Biology. 2012 Jan 1;61(1):170–3.

83. Chen S, Zhou Y, Chen Y, Gu J. fastp: an ultra-fast all-in-one FASTQ preprocessor. Bioinformatics. 2018 Sep 1;34(17):i884–90.

84. Wick RR, Judd LM, Cerdeira LT, Hawkey J, Méric G, Vezina B, et al. Trycycler: Consensus Long-read Assemblies for Bacterial Genomes. Genome Biology. 2021 Sep 14;22(1):266.

85. Wick RR, Judd LM, Gorrie CL, Holt KE. Unicycler: Resolving Bacterial Genome Assemblies From Short and Long Sequencing Reads. PLOS Computational Biology. 2017;13(6):e1005595.

86. Wick RR, Schultz MB, Zobel J, Holt KE. Bandage: interactive visualization of de novo genome assemblies. Bioinformatics. 2015 Oct 15;31(20):3350–2.

87. Schwengers O, Jelonek L, Dieckmann MA, Beyvers S, Blom J, Goesmann A. Bakta: rapid and standardized annotation of bacterial genomes via alignment-free sequence identification. Microb Genom. 2021 Nov 5;7(11):000685.

88. Alikhan NF, Petty NK, Ben Zakour NL, Beatson SA. BLAST Ring Image Generator (BRIG): Simple Prokaryote Genome Comparisons. BMC Genomics. 2011;12(1):402.

89. Robertson J, Nash JHEY. MOB-suite: Software Tools for Clustering, Reconstruction and Typing of Plasmids from Draft Assemblies. Microbial Genomics. 2018;4(8):e000206.

90. Siguier P, Perochon J, Lestrade L, Mahillon J, Chandler M. ISfinder: The Reference Centre for Bacterial Insertion Sequences. Nucleic acids research. 2006;34:D32–6.

91. Sullivan MJ, Petty NK, Beatson SA. Easyfig: a genome comparison visualizer. Bioinformatics. 2011 Apr 1;27(7):1009–10.

92. Tonkin-Hill G, MacAlasdair N, Ruis C, Weimann A, Horesh G, Lees JA, et al. Producing Polished Prokaryotic Pangenomes with the Panaroo Pipeline. Genome Biology. 2020;21(1):180.

ACKNOWLEDGEMENTS

We thank all staff members of the Enterics and MDDI section at the Microbiological Diagnostic Unit Public Health Laboratory (MDU PHL) for their technical assistance. We would also like

940 to thank Jake Lacey for his assistance uploading the reads to NCBI. The BEAST analysis for
941 this paper was undertaken using the LIEF HPC-GPGPU Facility hosted at the University of
942 Melbourne. This Facility was established with the assistance of LIEF Grant LE170100200.
943

944 **AUTHOR INFORMATION**

945 These authors contributed equally: Deborah A Williamson, Jaclyn S Pearson, Danielle J Ingle
946

947 **Authors and Affiliations**

948 **Department of Microbiology and Immunology, The University of Melbourne at The Peter**
949 **Doherty Institute for Infection and Immunity, Melbourne, Victoria, Australia.**

950 Cheryll M Sia, Benjamin P Howden, Danielle J Ingle
951

952 **Centre for Innate Immunity and Infectious Diseases, Hudson Institute of Medical**
953 **Research, Clayton, Melbourne, VIC, Australia.**

954 Rebecca Ambrose, Jaclyn S Pearson
955

956 **Department of Infectious Diseases, The University of Melbourne at the Peter Doherty**
957 **Institute for Infection and Immunity, Melbourne, VIC, Australia.**

958 Deborah A Williamson
959

960 **Microbiological Diagnostic Unit Public Health Laboratory, Department of Microbiology**
961 **& Immunology, The University of Melbourne at The Peter Doherty Institute for Infection**
962 **and Immunity, Melbourne, Victoria, Australia.**

963 Cheryll M Sia, Mary Valcanis, Patiyan Andersson, Susan A Ballard, Benjamin P Howden
964

Department of Microbiology, Monash University, Clayton, Victoria, Australia.

Jaclyn S Pearson

School of Medicine, University of St Andrews, St Andrews, Fife, Scotland.

Jaclyn S Pearson

Contributions

Study design and oversight: CMS, RA, DAW, JSP, DJI. Isolate collection and metadata: MV, PA, SAB, BJP. Performed wet lab experiments: RA, JSP. Data analysis: CMS, RA, JSP, DJI. Manuscript writing: CMS, RA, DAW, JSP, DJI. All authors contributed to manuscript editing.

ETHICS DECLARATIONS

Competing interests

The authors declare no competing financial interests.

981 **Figures and Tables**

982

983 **Figure 1. Overview of *S.* Dublin genomes in study**

984 Geographical distribution and clonal relationship of 1,303 *S.* Dublin genomes in the study. A)
985 Number of *S*. Dublin genomes according to geographical region and time interval of collection.
986 B) Distribution of human, animal and food *S*. Dublin genomes collected over time. C)
987 Distribution of *S*. Dublin sequence types (ST) from each region. Each coloured circle correlates
988 to an ST. Circles in green indicate no ST was identified. D) Unrooted phylogenetic tree of 1,303
989 *S.* Dublin genomes. Two main lineages of ST74 (n=8) and ST10 (n=1,295) shown in blue and
990 pink respectively. E) Relatedness of known sequence types (STs) to ST10. The nodes are
991 labelled with the ST and the branch lengths are indicative of the number of dissimilar locus
992 variants to ST10.

993

994

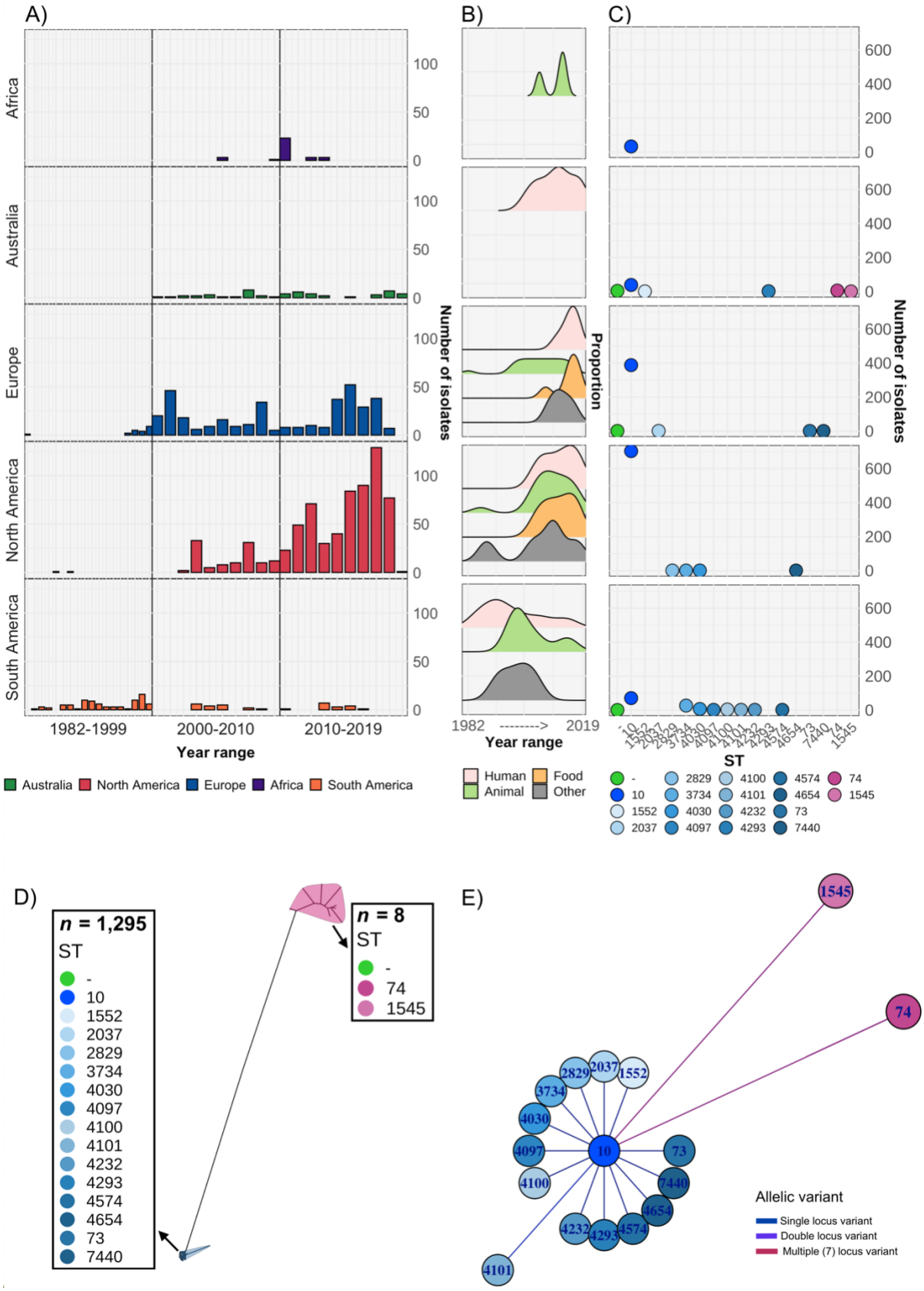
A)
B)
C)
Africa
Australia
Europe
North America
South America
Number of isolates
Proportion
1982-1999
2000-2010
2010-2019
Year range
1982 -------> 2019
Year range
ST
Australia North America Europe Africa South America
Human Food
Animal Other
- 10 1552 2037 2829 3734 4030 4097 4100 4101 4232 4293 4574 4654 73 7440 74 1545
D)
n = 1,295
ST
-
10
1552
2037
2829
3734
4030
4097
4100
4101
4232
4293
4574
4654
73
7440
n = 8
ST
-
74
1545
E)
Allelic variant
Single locus variant
Double locus variant
Multiple (7) locus variant

998 **Figure 2. Estimation of divergence time**

999 Maximum clade credibility (MCC) tree of the 667 *S.* Dublin ST10 genomes. The time in years
1000 is shown on the x-axis. From left to right, the coloured heatmaps refer to the region of origin,
1001 the susceptibility profile, the BAPs clade, and the presence of IncC and IncN plasmid types.
1002 The green dot denotes the most recent common ancestor (MRCA) of the Australian subclade,
1003 while the maroon dot represents the MRCA of clade 5 MDR isolates from North America.
1004 Internal nodes coloured chestnut red have a posterior probability ≥ 0.95.

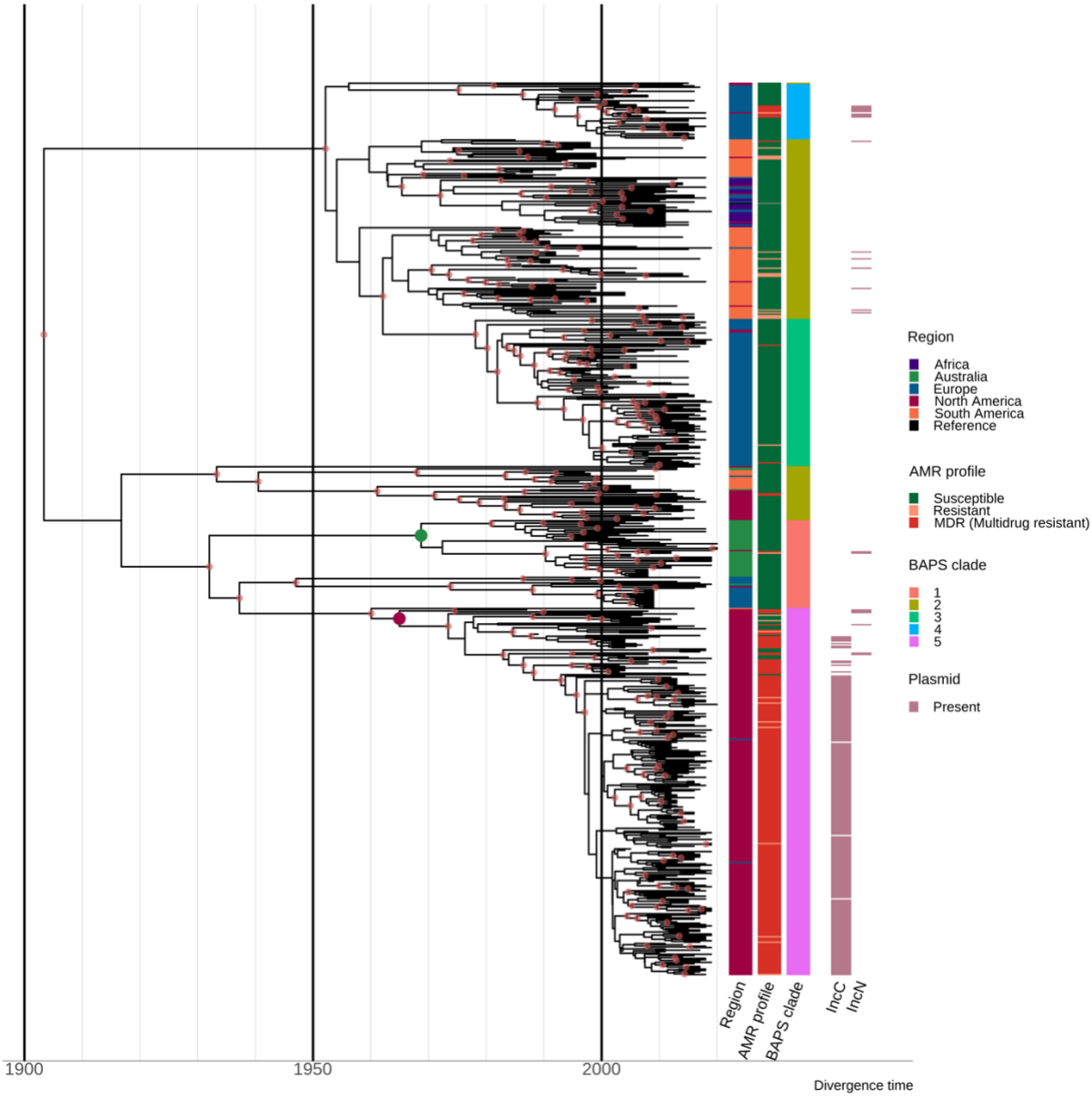

1005

1006

Figure 3. Resistance profiles of *S.* Dublin genomes

Observed resistance profiles of *S.* Dublin genomes spanning three-time intervals for each region. A) Frequency of susceptible and resistant *S.* Dublin genomes from each time period B) Antimicrobial resistance profiles observed spanning three time periods. The colour of the circle corresponds to an antimicrobial class, while the height is relative to the number of genomes. C) Heavy metal and biocide resistance profiles observed. The colour of the circle corresponds to its respective heavy metal/biocide class, while the height is relative to the number of genomes.

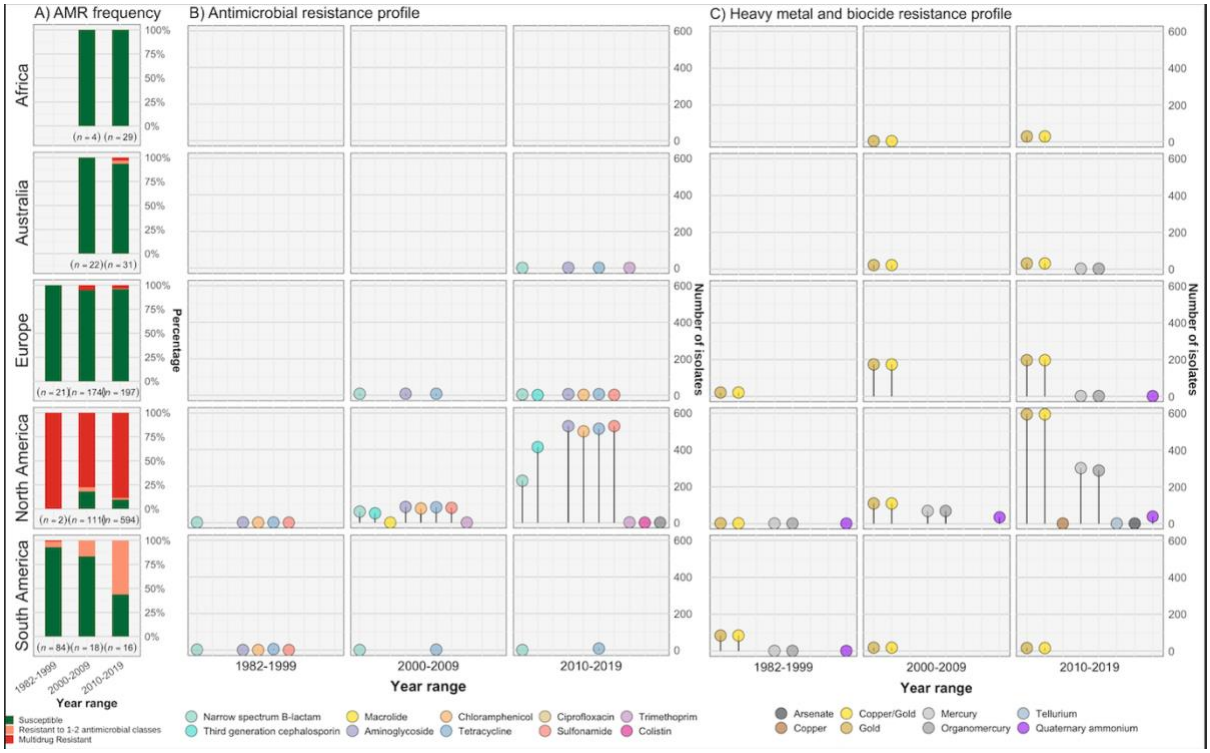

1020 **Figure 4. Invasive factors associated with *S.* Dublin genomes**

1021 Correlation of *Salmonella* pathogenicity islands (SPIs) to *S.* Dublin's invasiveness. A)
1022 Validation of the likelihood of invasiveness prediction tool using a variety of publicly available
1023 genomes consisting of non-invasive and invasive *Salmonella* serovars (Supplementary Table
1024 8). B) The correlation of index scores to the source and its sequence type based on the region.
1025 * indicates a statistically significant p-value between the index scores of two sources. C)
1026 Chromosomal assemblies of ST10 (blue) and ST74 (pink) genomes aligned to *S.* Dublin
1027 chromosomal reference CT_02021853 (CP001144.1) with a lower limit of 80% identity D)
1028 Aligned sequence of SPI-6 region of an ST10, AUSMDU00056868, and an ST74,
1029 AUSMDU00016676, in comparison to SPI-6 region of reference CT_02021853. E) Aligned
1030 sequence of SPI-19 region of an ST10, AUSMDU00056868, and an ST74,
1031 AUSMDU00016676 in comparison to SPI-19 region of reference CT_02021853.

1032 SPI, *Salmonella* pathogenicity island.

1033

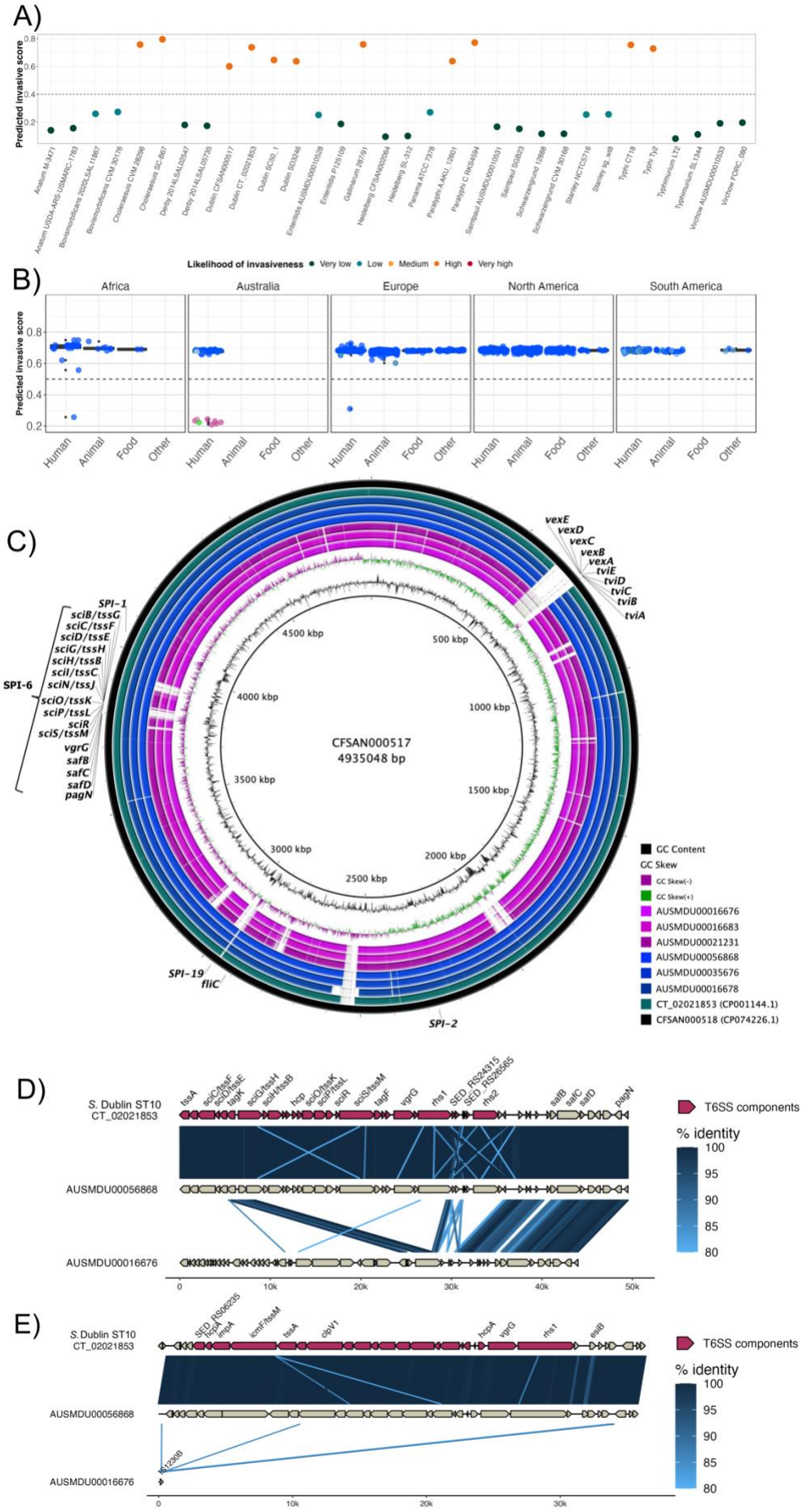
A)
Predicted invasive score
Likelihood of invasiveness
Very low
Low
Medium
High
Very high
B)
Africa
Australia
Europe
North America
South America
Predicted invasive score
Human
Animal
Food
Other
C)
vexE
vexD
vexC
vexB
vexA
tviE
tviD
tviC
tviB
tviA
SPI-1
sciB/tssG
sciC/tssF
sciD/tssE
sciG/tssH
sciH/tssB
sciI/tssC
sciN/tssJ
SPI-6
sciO/tssK
sciP/tssL
sciR
sciS/tssM
vgrG
safB
safC
safD
pagN
4500 kbp
500 kbp
4000 kbp
1000 kbp
CFSAN000517
4935048 bp
3500 kbp
1500 kbp
3000 kbp
2000 kbp
2500 kbp
SPI-19
fliC
SPI-2
GC Content
GC Skew
GC Skew(-)
GC Skew(+)
AUSMDU00016676
AUSMDU00016683
AUSMDU00021231
AUSMDU00056868
AUSMDU00035676
AUSMDU00016678
CT_02021853 (CP001144.1)
CFSAN000518 (CP074226.1)
D)
S. Dublin ST10
CT_02021853
tssA
sciC/tssF
sciD/tssE
tagK
sciG/tssH
sciH/tssB
hcp
sciO/tssK
sciP/tssL
sciR
sciS/tssM
tagF
vgrG
rhs1
SED_RS4315
SED_RS26565
rhs2
safB
safC
safD
pagN
AUSMDU00056868
AUSMDU00016676
0
10k
20k
30k
40k
50k
T6SS components
% identity
100
95
90
85
80
E)
S.Dublin ST10
CT_02021853
SED_RS06235
hcpA
impA
iomF/tssM
tssA
clpV1
hcpA
vgrG
rhs1
eaiB
AUSMDU00056868
AUSMDU00016676
0
10k
20k
30k
T6SS components
% identity
100
95
90
85
80

1034

1035

1036 **Figure 5. *S.* Dublin ST74 isolates demonstrate increased intracellular replication in**
1037 **human macrophages over ST10 isolates**

1038 Differentiated THP-1 (human monocyte) cells were infected at an MOI:10 with selected ST10
1039 and ST74 *S.* Dublin isolates. **A, B)** THP-1 cells were lysed, and intracellular bacteria
1040 enumerated as fold change in replication and **C-F)** CFU/well at time 0, 3, 9 and 24 hpi. For **A)**,
1041 each measurement at times 3, 9 and 24 hpi represents the fold change in CFU/well compared
1042 to 0 hpi, the start of infection, recorded as a biological replicate (performed in technical
1043 triplicate), with error bars indicating ± 1 standard deviation of n = 3 biological replicates. For
1044 **C-D**), each dot represents CFU/well of a biological replicate (performed in technical triplicate),
1045 with error bars indicating ± 1 standard deviation of n = 3 biological replicates. Statistical
1046 significance was determined by nested student's t-test. MOI, multiplicity of infection, hpi,
1047 hours post-infection, CFU, colony-forming units, FC, fold-change.

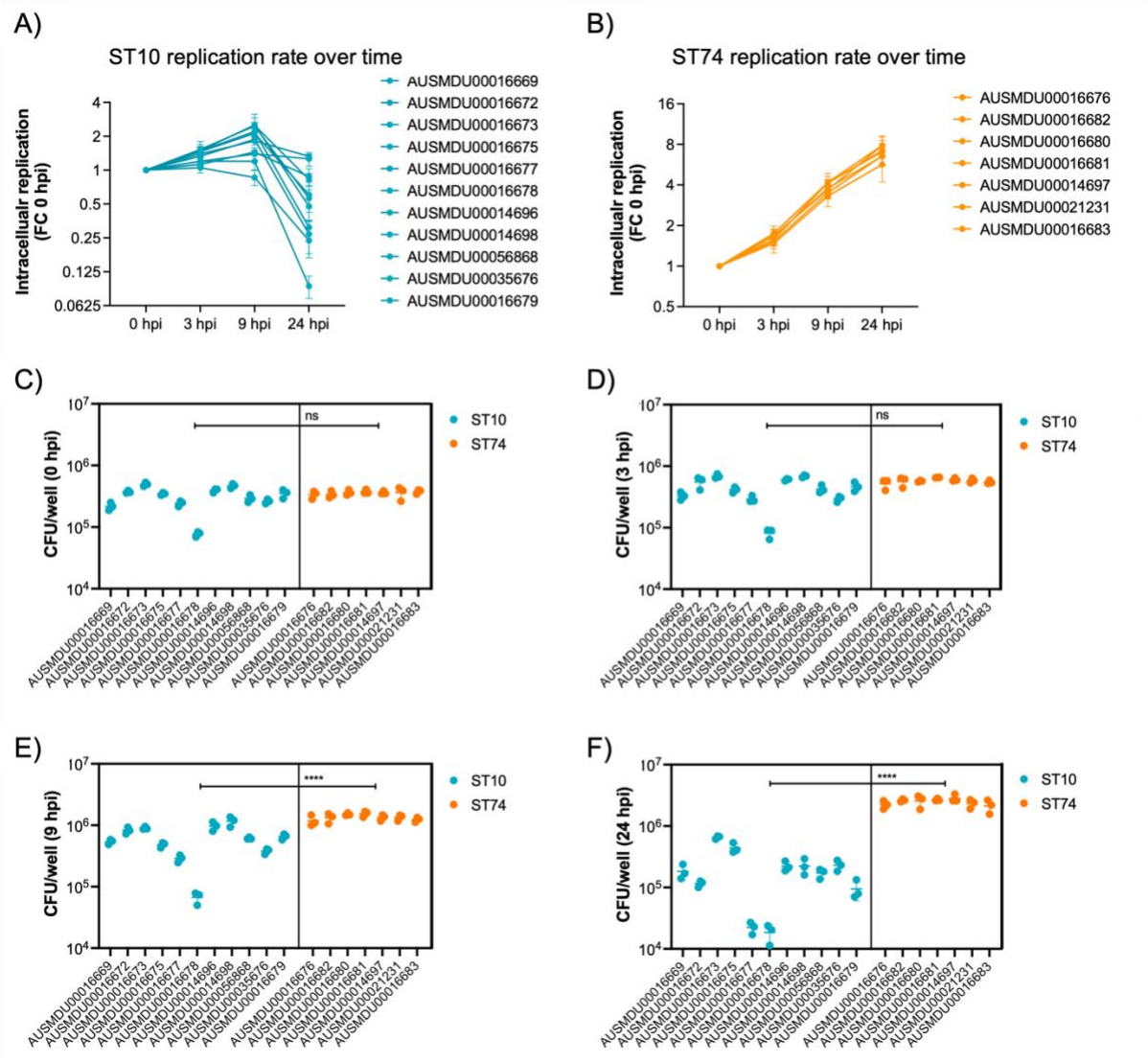

1048

1049

1050

1051 **Figure 6. *S.* Dublin ST74 isolates induce comparable cytotoxicity to ST10 isolates in**
1052 **human macrophages, despite increased intracellular growth**

1053 **A-C)** Cell supernatants were assayed for LDH as a measure of cytopathic effects of infection,
1054 and % cytotoxicity was calculated by comparison with 100% lysed uninfected control cells.
1055 Samples were collected from THP-1 cells at 3, 9 and 24 hpi. Each point represents the %
1056 cytotoxicity of a biological replicate (performed in technical triplicate), with error bars
1057 indicating ± 1 standard deviation of n = 3 biological replicates. Statistical significance was
1058 determined by nested student's t-test. **D)** IL-1ß secretion from THP-1 cells infected for 9 hours
1059 with *S.* Dublin isolates. Error bars indicate ± 1 standard deviation of n = 3 biological replicates
1060 and statistical significance determined by student's t-test **E)** Immunoblot of cleaved IL-1ß
1061 (Asp166) in THP-1 cell lysates infected with *S.* Typhimurium reference strain SL1344,
1062 *S.* Dublin ST10 (AUSMDU00016673), or *S.* Dublin ST74 (AUSMDU00016682) over 0, 3, 8
1063 and 24 hours. **F)** Scatter plot comparing replication rate, % cytotoxicity and IL-1β secretion
1064 from THP-1 cells infected with *S.* Dublin isolates at 9 hpi. Each dot represents each biological
1065 replicate of three (averaged from three technical replicates). MOI, multiplicity of infection, hpi,
1066 hours post-infection, CFU, colony-forming units, LDH, lactate dehydrogenase.

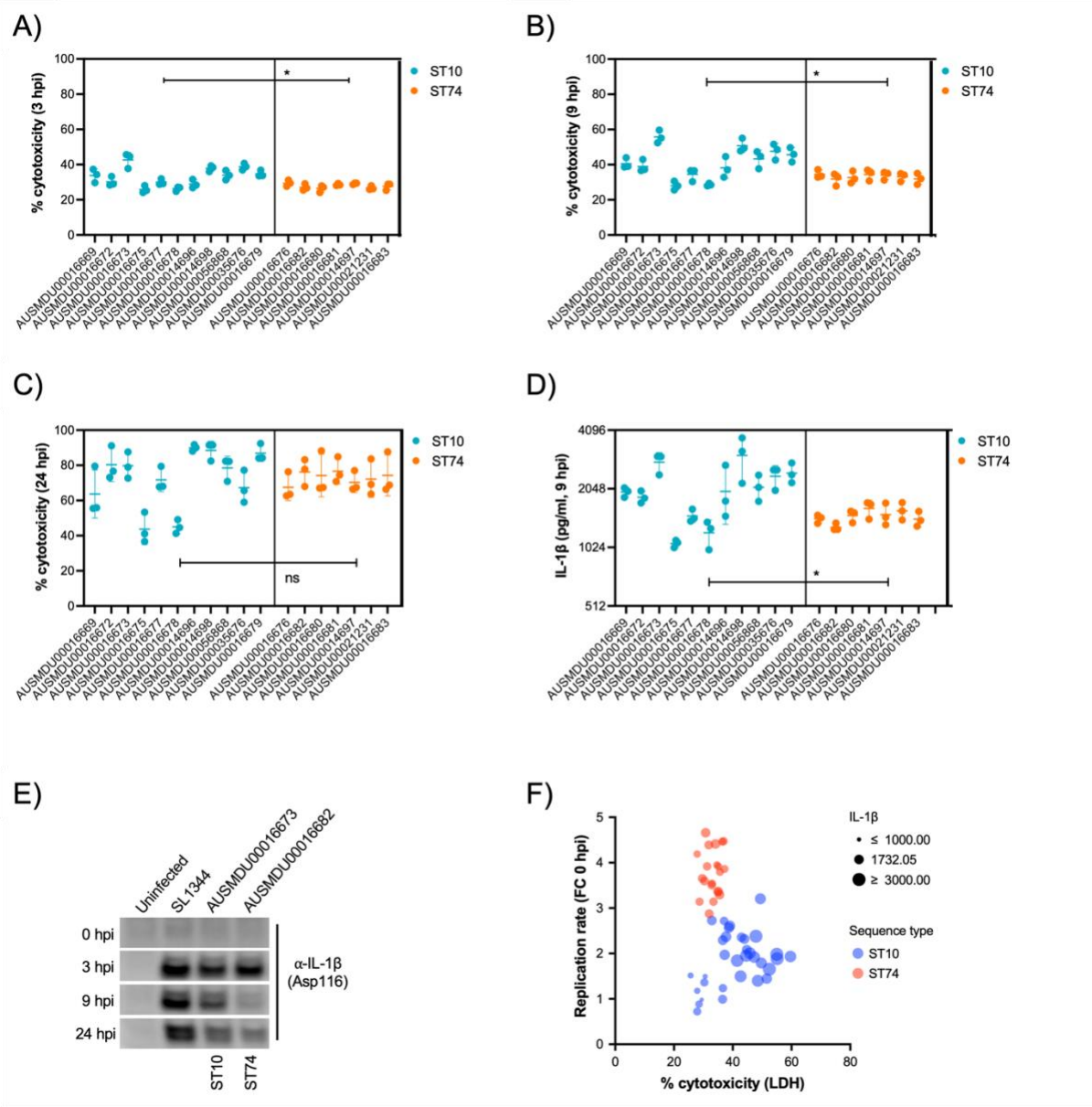
A)
% cytotoxicity (3 hpi)
ST10
ST74
*
B)
% cytotoxicity (9 hpi)
ST10
ST74
*
C)
% cytotoxicity (24 hpi)
ST10
ST74
ns
D)
IL-1β (pg/ml, 9 hpi)
ST10
ST74
*
E)
Uninfected
SL1344
AUSMDU00016673
AUSMDU00016682
0 hpi
3 hpi
9 hpi
24 hpi
α-IL-1β
(Asp116)
ST10
ST74
F)
Replication rate (FC 0 hpi)
% cytotoxicity (LDH)
IL-1β
≤ 1000.00
1732.05
≥ 3000.00
Sequence type
ST10
ST74

1067